

# Biodegradation of polyethylene terephthalate by *Tenebrio molitor*: Insights for polymer chain size, gut metabolome and host genes

Lei He<sup>a,b</sup>, Shan-Shan Yang<sup>b,\*</sup>, Jie Ding<sup>b</sup>, Cheng-Xin Chen<sup>b</sup>, Fan Yang<sup>c</sup>, Zhi-Li He<sup>d</sup>, Ji-Wei Pang<sup>e</sup>, Bo-Yu Peng<sup>f</sup>, Yalei Zhang<sup>f</sup>, De-Feng Xing<sup>b</sup>, Nan-Qi Ren<sup>b</sup>, Wei-Min Wu<sup>g,\*</sup>

<sup>a</sup> CAS Key Laboratory of Urban Pollutant Conversion, Department of Environmental Science and Engineering, University of Science and Technology of China, Hefei 230026, China

<sup>b</sup> State Key Laboratory of Urban Water Resource and Environment, School of Environment, Harbin Institute of Technology, Harbin 150090, China

<sup>c</sup> School of Life Science and Technology, Harbin Institute of Technology, Harbin 150090, China

<sup>d</sup> Southern Marine Science and Engineering Guangdong Laboratory (Zhuhai), Zhuhai 519080, China

<sup>e</sup> China Energy Conservation and Environmental Protection Group, Beijing 100089, China

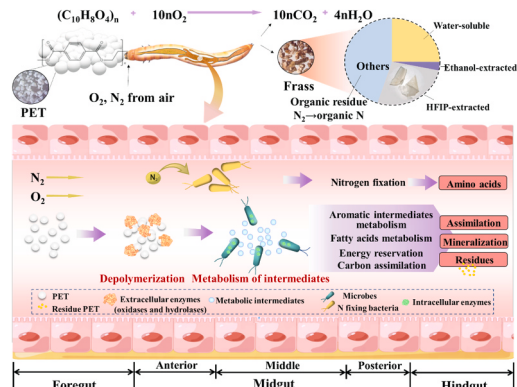
<sup>f</sup> State Key Laboratory of Pollution Control and Resource Reuse, College of Environmental Science and Engineering, Tongji University, Shanghai 200092, China

<sup>g</sup> Department of Civil and Environmental Engineering, William & Cloy Codiga Resource Recovery Center, Stanford University, Stanford, CA 94305, USA

## HIGHLIGHTS

- High-crystallinity PET biodegradation was confirmed by testing change of  $\delta^{13}\text{C}$ .
- Depolymerization is independent of gut microbes.
- Polymer molecular size influences degradation rates.
- Gut microbiomes synergistically biodegrade intermediates and provide nitrogen sources.
- Upregulation of host genes for PET depolymerization and metabolism.

## GRAPHICAL ABSTRACT



## ARTICLE INFO

**Keywords:**  
Polyethylene terephthalate

## ABSTRACT

Polyethylene terephthalate (PET or polyester) is a commonly used plastic and also contributes to the majority of plastic wastes. Mealworms (*Tenebrio molitor* larvae) are capable of biodegrading major plastic polymers but their

**Abbreviations:** ABC, ATP binding cassette; BD, Broad extent depolymerization; CAZy, Carbohydrate-active enzymes; CDS, Coding regions; CFU, Colony forming units; GO, Gene ontology; FA, Fatty acid; FT-IR, Fourier transform infrared spectroscopy; GPC, Gel permeation chromatography; HFIP, 1,1,1,3,3-hexafluoroisopropanol;  $^1\text{H}$  NMR,  $^1\text{H}$  nuclear magnetic resonance; KEGG, Kyoto encyclopedia of genes and genomes; LD, Limited extent depolymerization; LDPE, Low-density polyethylene; LEfse, Linear discriminant analysis effect size; MHET, Monohydroxyethyl terephthalate; MPs, Microplastics;  $M_n$ , Number-average molecular weight;  $M_w$ , Weight-average molecular weight; MW, Molecular weight; MWD, Molecular weight distribution;  $M_z$ , Size-average molecular weight; NPs, Nanoplastics; PCoA, Principal coordinate analysis; PE, Polyethylene; PET, Polyethylene terephthalate; PLA, Polylactic acid; PP, Polypropylene; PS, Polystyrene; PUR, Polyurethane; PVC, Polyvinyl chloride; SR, Survival rate;  $\delta^{13}\text{C}$ , Stable carbon isotopes; TCA cycle, Tricarboxylic acid cycle; WB, Wheat bran.

\* Corresponding authors.

E-mail addresses: [shanshanyang@hit.edu.cn](mailto:shanshanyang@hit.edu.cn) (S.-S. Yang), [billwu@stanford.edu](mailto:billwu@stanford.edu) (W.-M. Wu).

<https://doi.org/10.1016/j.jhazmat.2024.133446>

Received 18 August 2023; Received in revised form 2 January 2024; Accepted 3 January 2024

Available online 6 January 2024

0304-3894/© 2024 Elsevier B.V. All rights reserved.



Biodegradation  
*Tenebrio molitor*  
 Host transcriptome  
 Gut microbiome

degrading ability for PET has not been characterized based on polymer chain size molecular size, gut microbiome, metabolome and transcriptome. We verified biodegradation of commercial PET by *T. molitor* larvae in a previous report. Here, we reported that biodegradation of commercial PET ( $M_w$  29.43 kDa) was further confirmed by using the  $\delta^{13}\text{C}$  signature as an indication of bioreaction, which was increased from  $-27.50\text{\textperthousand}$  to  $-26.05\text{\textperthousand}$ . Under antibiotic suppression of gut microbes, the PET was still depolymerized, indicating that the host digestive enzymes could degrade PET independently. Biodegradation of high purity PET with low, medium, and high molecular weights (MW), i.e.,  $M_w$  values of 1.10, 27.10, and 63.50 kDa with crystallinity 53.66%, 33.43%, and 4.25%, respectively, showed a mass reduction of  $>95\%$ , 86%, and 74% via broad depolymerization. Microbiome analyses indicated that PET diets shifted gut microbiota to three distinct structures, depending on the low, medium, and high MW. Metagenome sequencing, transcriptomic, and metabolic analyses indicated symbiotic biodegradation of PET by the host and gut microbiota. After PET was fed, the host's genes encoding degradation enzymes were upregulated, including genes encoding oxidizing, hydrolyzing, and non-specific CYP450 enzymes. Gut bacterial genes for biodegrading intermediates and nitrogen fixation also upregulated. The multiple-functional metabolic pathways for PET biodegradation ensured rapid biodegradation resulting in a half-life of PET less than 4 h with less negative impact by PET MW and crystallinity.

## 1. Introduction

Polyethylene terephthalate (PET) is a ubiquitous plastic that is commonly known as “polyester” in the textile industry. PET products belong to aromatic polyesters, expressed as  $(\text{C}_{10}\text{H}_8\text{O}_4)_n$  and consisting of polymerized units of monohydroxyethyl terephthalate (MHET). When used in textile-grade products, PET generally has an average molecular weight (MW) of about 20.00 kDa, while commercial PET products have 8.00 to 31.00 kDa of the weight-average molecular weight ( $M_w$ ) [1]. Annually, about 70 million tons of PET are produced for packaging and textiles with only a small fraction (<20%) of that amount being recycled [2,3]. Consequently, PET pollution has been an environmental concern for years [4,5]. The degradation rate is extremely slow with a time frame of months to years. Some researchers predicted the general life time of PET to range from 16 to 48 years in the environment [6].

Since the last decade, a number of PET-degrading bacterial and fungal cultures have been enriched and isolated from environments to help researchers investigate PET biodegradation. The results have shown to be promising [7–9]. Enzymatic PET degradation has achieved significant progress [5]. Nowadays, PET hydrolases from bacteria such as Actinomycetota phylum, Pseudomonadota phylum, and Bacteriodota phylum, as well as several fungi have been tested and engineered to decompose recycled PET [10,11]. Industrial-scale PET recycling based on enzymatic hydrolysis is underway, however, several technical (low efficient of monomer recovery, low prevalence of activity, low thermal and pH stability, impact of PET properties, e.g., crystallinity, particle size, etc., enzymatic properties and stability), engineering, and economic challenges still remain to be solved [7,10,12]. Furthermore, under ambient temperatures, research on PETase, MHETase, and cutinase remains limited to that of processing monomers or low-crystallinity/amorphous PET [10,13]. PET products for bottles and textiles are associated with high crystallinity of 30–40%, which restricts the rate of enzymatic degradation [10,12,13]. For example, the half-life of high crystallinity PET (35%,  $M_w$  35.00 kDa) was still 372 hr with the treatment of leaf compost-cutinase enzyme (LCC-ICCG) [13].

Since 2015, insects belonging to families of the darkling beetles (*Tenebrionidae*) and pyralid moths (*Pyralidae*) have been found to be capable of biodegrading plastics [5,14–25]. Yellow mealworms, the larvae of *Tenebrio molitor* Linnaeus 1758, are observed around the world, and are naturally present in forests with rotting wood, where they eat dried leaves and lignocellulosic materials [26]. Mealworms are commercialized as animal feed all over the world and have also been suggested for use as a potential sustainable replacement for food protein for both human and animal consumption [27]. Mealworms have been found to have the novel ability to biodegrade polystyrene (PS) [28–30], polyethylene (PE) [31–34], polyvinyl chloride (PVC) [34,35], polypropylene (PP) [34,35], polyurethane (PUR) [36], and polylactic acid (PLA) [37]. Recently, we confirmed biodegradation of two commercial PET polymers with  $M_w$  of 39.33 and 29.43 kDa, and a crystallinity of

22.80% and 18.00%, respectively, resulting in an average mass reduction of 71.03% and 73.28% [38].

Physicochemical properties of polymers impact the biodegradation rate of plastics, with major factors including polymer type, surface hydrophobicity, molecular weight distribution (MWD), and three dimensional structure (e.g. crystallinity) [39]. Research results indicated that low-density PE (LDPE) and PS depolymerization and biodegradation by *T. molitor* was significantly impacted by polymer MW [29,33]. For PS and LDPE, polymers with the low and medium MW are biodegraded via broad extent depolymerization (BD) pattern. Similar BD patterns were also observed in our previous study on biodegradation of two commercial PET polymers by *T. molitor* larvae [38]. However, when PS and PE with high or extremely high MW were fed, a limited extent depolymerization (LD) pattern occurred, i.e., increase in  $M_n$  or  $M_w$  or both, indicating that polymers with high MW accumulated or are degraded at a much slower rate than polymers with lower MW [32,40]. It is unknown if different depolymerization patterns could also occur during biodegradation of commercial PET products with a higher MW than that of the two products tested [38].

The biodegradation of PET has been characterized through the identification of formation oxidized groups using Fourier transform infrared spectroscopy (FT-IR) and  $^1\text{H}$  nuclear magnetic resonance ( $^1\text{H}$  NMR) [38], which are two tools commonly used for the characterization of biodegradation of PE, PP, PS, and PVC [40]. In this study, we tested the use of stable carbon isotope ( $\delta^{13}\text{C}$ ) values of residual PET as an indication for demonstrating PET biodegradation. This method is based on the fact that during biodegradation, organisms preferentially take up light  $^{12}\text{C}$ , and thus, the  $^{13}\text{C}$  isotope in residual organic compounds increases. Monitoring stable isotope ratio has been successfully applied for several biodegradation tests, e.g., in vitro biodegradation of hydrocarbon vapor [41], and reductive dechlorination of trichloroethylene [42]. To date, this method has barely been applied for measuring the plastic biodegradation ability of *T. molitor* and other insects when it comes to PET.

Previous studies indicated that biodegradation of distinct plastics in *T. molitor* larvae implied a complexity of mechanisms [16,32,43]. The gut microbes are involved in plastics biodegradation, particularly depolymerization. Biodegradation of PE by *T. molitor* and *G. mellonella* did not stop even under antibiotic depression conditions [15,44], whereas the depolymerization and biodegradation of PS and PVC stopped or was severely inhibited under antibiotic suppression of gut microbes [16,28,32]. As for PET biodegradation, to date, the contribution of the gut microbiota and the symbiotic mechanism has not yet been described in details. To date, limited research has been done on the digestive enzymes secreted during plastic degradation by gut microbes and the insect hosts, i.e., *T. molitor*, *Z. atratus*, and *G. mellonella* [15,19,45,46], and such PET degradation mechanism remain unclear.

In the environment, the host and associated microbes within the intestine commonly cooperate and interact, eventually forming an

intimate symbiotic relationship [47]. Recent studies on microbiome during PS biodegradation suggested that the plastics-degrading gut microbes originated from the insects' ancient or natural diets, which contain lignocellulosic materials [48].

Based on previous studies described above, for biodegradation of PET in *T. molitor* larvae, we hypothesized: a) selective isotopic exchange between  $^{12}\text{C}$  and  $^{13}\text{C}$  occurred to enrich  $^{13}\text{C}$  in residual PET; b) antibiotic suppression might have less impact on PET depolymerization than on non-hydrolysable polymers such as PS, LDPE, etc.; c) the phenotypic characteristics of the larvae, such as growth state, environmental adaptation, and PET degradation characteristics were closely interconnected with gut microbiome; d) the community structure and metabolic activities of intestinal microbes were impacted by physical properties of the PET polymers, especially MW; and e) the gut microbiota contributes to the digestion of ingested plastics with a supplementation of organic nutrients, especially nitrogen sources.

In this report, we aimed to use PET with three different MWs to examine the aforementioned five hypotheses in order to advance our understanding of the PET degradation mechanism by the associated gut microbiome. We characterized the commercial PET depolymerization with stable isotopic signatures and the impact of antibiotic suppression, and examined the impact of polymer MW on PET degradation, intestinal microbiome, host transcriptome, and intestinal metabolome.

## 2. Materials and methods

### 2.1. *T. molitor* Larvae, PET materials, chemicals and feedstock preparation

*T. molitor* larvae ( $27.13 \pm 0.50$  mg/larva) were obtained from a breeding farm in Dezhou, Shandong, China. They were fed with wheat bran (WB) prior to testing.

Commercial grade PET microplastics (MPs) powders (< 75.00  $\mu\text{m}$ , crystallinity:  $18.00\% \pm 2.25\%$ ) were purchased from Zhongxin Plastic Factory (Guangdong, China), which was also used in previous studies [38] (Fig. S1a). The PET did not contain toxic additives or catalysts. Three high purity PET powders (chromatographically pure as standard) with respective  $M_w$  of 1.10, 27.10, and 63.50 kDa,  $M_n$  of 0.86, 15.40, and 30.00 kDa, and crystallinity  $53.66\% \pm 3.31\%$ ,  $33.43\% \pm 3.01\%$ , and  $4.25\% \pm 1.64\%$ , represented low, medium, and high MW PET polymers, which were named PET<sub>1100</sub>, PET<sub>27100</sub>, and PET<sub>63500</sub> in this study. PET<sub>1100</sub> was irregularly shaped solid bulk material. PET<sub>27100</sub> was fine powder (around 60.00  $\mu\text{m}$ ) and PET<sub>63500</sub> were pellets with a size of 2.00–4.00 mm (Fig. S1b). These samples were purchased from the American Polymer Standards Corporation. The PET<sub>1100</sub> and PET<sub>63500</sub> samples were grinded to reduce particular size to less than 75.0  $\mu\text{m}$  prior to use. They were soaked in a liquid nitrogen bath for about 5 min and then mechanically grinded by a stainless steel high-throughput tissue grinder (Wonbio-L, Shanghai Wonbio Biotechnology co., Ltd, Shanghai). Five types of antibiotics, including aminoglycosides, macrolides, amphenicol, tetracycline, and  $\beta$ -lactam antibiotics, i.e., gentamicin sulfate, erythrocine, chloramphenicol, tetracycline, ampicillin, and kanamycin were purchased from Biotopped Co. (Beijing, China). They were mixed together for the suppression of gut bacteria.

WB was purchased from the same farm where the larvae were purchased, a breeding farm in Dezhou, Shandong, China. Agar was purchased from Aoboxing Biotechnology Co., Ltd (Beijing). All other chemicals were purchased from Macklin (Shanghai, China).

### 2.2. Biodegradation of PET in *T. molitor* larvae

Before the test, the larvae were kept unfed for 24 h to allow for digestion of previous feedstock. Then, they were reared with different diets in food-grade PP containers in an artificial climate incubator (Shanghai Shuli, Shanghai, China) under stable conditions (25 °C, 70% relative humidity, in the dark). All treatment groups were conducted in

triplicate.

The test for biodegradation of commercial PET was performed with 500 larvae in each incubator (16 × 11 × 5 cm) [38]. Three feeding conditions were employed: a) PET-fed; b) agar-fed; and c) unfed. The PET-fed larvae were fed with PET-agar gel (5:2, w/w) containing 5 g PET as the primary diet for 36 days. The agar-fed and unfed groups were designated as agar-fed and starvation controls. The larvae in the agar-fed control were fed with 2% (agar: DI water, w/vol) agar gel. This method was previously used for the biodegradation of PVC and PLA powders [16,37]. Initially, 3 g of PET-agar gel or agar gel (on wet weight basis) was supplied to the incubators. Subsequently, the diets were supplemented daily based on their consumption rate. The supplemented mass was recorded to calculate the total consumption at the end of the test. The frass was collected to extract residual PET polymers for the analysis of  $^{13}\text{C}/^{12}\text{C}$  ratio at the end of the test.

### 2.3. Effect of antibiotic suppression

Antibiotic suppression tests were designed to examine the contribution of gut microbiota in the presence of severe inhibition of gut microbes. At first, the larvae (500) were fed with commercial PET-agar gel for two weeks. Afterward, PET-agar (5:2, w/w) with an equal proportion of the mixed five antibiotics i.e., gentamicin sulfate, erythrocine, chloramphenicol, tetracycline, ampicillin, and kanamycin (0.075 mg/mg mixed antibiotics-agar) was prepared. The larvae were reared with the above diet for 5 days and then sampled to count gut bacterial numbers. Ten active larvae from each group were randomly selected and euthanized under sterile conditions. The gut tissues were collected, suspended, and homogenized in a 10% phosphate buffered saline solution with a ratio of 1:50 (w/vol). The suspension was plated (dilution factors varied from  $10^{-1}$  to  $10^{-3}$ ) on a plate counting medium (medium composition in Supporting Information (SI) M1) to count the number of bacterial colony forming units (CFUs). After five days, no CFUs were found in the plated gut suspensions from antibiotic-treated larvae. The larvae in the incubators were fed with the antibiotics containing PET-agar gel for another two weeks in order to examine PET degradation under antibiotic suppression versus PET degradation by the antibiotics-free control larvae.

### 2.4. Effect of PET MW on biodegradation

The effect of MW on PET degradation was performed to determine the consumption of three high purity PET-agar gels with 60 larvae (SI M2). The incubation ended when the feedstocks were consumed completely. This period lasted 13 days, 15 days, and 16 days for PET<sub>1100</sub>, PET<sub>27100</sub>, and PET<sub>63500</sub>, respectively, while lasting 11 days for WB. The weight changes and survival rates of the larvae, as well as the utilization rate and depolymerization/biodegradation of PET by the larvae, were recorded at the end of the consumption duration.

### 2.5. Characterization of residual PET polymers in frass

The depolymerization/biodegradation of ingested PET was characterized by Gel permeation chromatography (GPC),  $\delta^{13}\text{C}$ , FT-IR, and  $^1\text{H}$  NMR according to established methods used in previous studies [33,37,40], with detailed characterization information in SI M3. X-Ray Diffraction (Panalytical Empyrean, Netherlands) was utilized to analyze the crystallinity of PET polymers (SI M3). Detection of the ratio of  $^{13}\text{C}/^{12}\text{C}$  of the residual plastics from the frass versus the virgin plastic PET in delta ( $\delta$ ) notation in parts per thousand (‰) was calculated as follows:

$$\delta^{13}\text{C}(\text{‰}) = \left[ \frac{(^{13}\text{C}/^{12}\text{C})_{\text{sample}}}{(^{13}\text{C}/^{12}\text{C})_{\text{standard}}} - 1 \right] \times 1000 \quad (1)$$

The  $\delta^{13}\text{C}$  value was calibrated by the international carbon isotope

standard Vienna Pee Dee Belemnite (VPDB). The overall precision of the  $^{13}\text{C}$  measurement was  $\pm 0.20\%$ .

## 2.6. High-throughput 16 S ribosomal RNA gene sequencing

To assess the PET biodegradation mechanisms in the intestinal tract of the larvae, gut tissues from larvae fed with the low, medium, and high MW PET diets versus the WB diet were collected, frozen with liquid nitrogen, and saved at  $-80^\circ\text{C}$  prior to omics analysis. Gut microbiome analysis was performed using high-throughput 16 S ribosomal RNA gene sequencing and metagenomic sequencing. For this, the collected samples were immediately rinsed with sterile water to remove soluble organic contaminates from the host. The larvae (25 in each group) were randomly selected in triplicate. The gut samples were sent to LC Bio Technology CO., Ltd (Hangzhou, China) for sequencing and analysis. DNA of gut microbiome samples was extracted using CTBA. The 16 S rRNA gene was amplified by primers V3-V4 region 341 F (5'-CCTACGGNGGCWGCAG-3') and 805 R (5'-GACTACHVGGGTATC-TAATCC-3'). High-throughput sequencing of bacterial 16 S rRNA genes was performed on the Illumina NovaSeq PE250 platform (Illumina NovaSeq PE250, Illumina Inc., San Diego, CA, USA).

## 2.7. Bioinformatic and statistical analysis of 16 S rRNA gene amplicon sequencing data

Quality filtering on the raw reads was performed according to the fqtrim (version 0.94). Chimeric sequences were filtered using Vsearch software (version 2.3.4). After dereplication using DADA2, Amplicon Sequence Variants (ASVs) feature table and feature sequences were obtained. Blast was used for sequence alignment, and the feature sequences were annotated with SILVA (Release 138) and NT-16S database for each representative sequence using a confidence threshold of 70%. Other diagrams were implemented using the R package (version 3.5.2).

Alpha diversity was applied in analyzing the complexity of gut bacterial species diversity for a sample through Chao1 and Shannon calculated with QIIME2. Beta diversity was analyzed by the PCoA to evaluate microbiome complexity between samples. The divergence between the two groups was compared by ANOSIM analysis. Differences among treatments were examined using a Kruskal-Wallis test. Differences were considered statistically significant at  $p < 0.05$ .

## 2.8. DNA Library construction and metagenomic sequencing

The DNA of gut microbiome samples for metagenomic sequencing was extracted by the E.Z.N.A.® Stool DNA Kit (D4015-02, Omega, Inc., USA). Sequencing library construction was completed by the TruSeq Nano DNA LT Library Preparation Kit (FC-121-4001, Illumina). DNA was fragmented by dsDNA Fragmentase (NEB, M0348S) via incubation at  $37^\circ\text{C}$  for 30 min. Library construction began with fragmented cDNA. Blunt-end DNA fragments were generated by combining fill-in reactions and exonuclease activity. Narrow size selection was performed by sample purification beads. Then, an A-base was added to the blunt ends of each strand for ligating to the indexed adapters. Each adapter contained a T-base overhang for ligating the adapter to the A-tailed fragmented DNA. These adapters contained the full complement of sequencing primer hybridization sites for single, paired-end, and indexed reads. Single or dual-index adapters were ligated to the fragments, and the ligated products were amplified with PCR. Library purification, quantification, and quality control was followed by high-throughput sequencing carried out on the NovaSeq6000 platform (Illumina) and 150 bp paired end reads were generated.

## 2.9. Bioinformatic analysis of metagenomic sequencing

Raw sequencing reads were processed to obtain valid reads for further analysis. In particular, sequencing adapters were removed from

sequencing reads using cutadapt v1.9. Then, a sliding-window algorithm was used to trim low quality reads by fqtrim v0.94. Next, reads were aligned to the host genome using bowtie2 v2.2.0 to remove host contamination. After quality-filtered reads were obtained, they were de novo assembled to construct the metagenome for each sample by IDBA-UD v1.1.1. All coding regions (CDS) of metagenomic contigs were predicted by MetaGeneMark v3.26.

CDS sequences of all samples were clustered by CD-HIT v4.6.1 to obtain unigenes. Unigene abundance for a certain sample was estimated by TPM based on the number of aligned reads by bowtie2 v2.2.0. The lowest common ancestor taxonomy of unigenes was obtained by aligning them against the NCBI NR database by DIAMOND v 0.9.14. Similarly, the functional annotation (Gene ontology (GO), Kyoto encyclopedia of genes and genomes (KEGG) of unigenes were obtained. Based on the taxonomic and functional annotation of unigenes, along with the abundance profile of unigenes, a differential analysis was carried out at each taxonomic, functional, or gene-wise level by a Kruskal-Wallis test.

## 2.10. Transcriptome analysis

All RNA of larval gut tissue including bacterial biomass was extracted using Trizol reagent (Thermo Fisher, 15596018) following the manufacturer's procedure. RNA quantity and quality were assessed by Bioanalyzer 2100 and RNA 6000 Nano LabChip Kit (Agilent, CA, USA) with RIN number  $> 7.0$ . Poly-T oligo-attached magnetic beads used to isolate poly (A) mRNA from collected total RNA. After purification, the poly(A)-or poly(A) + RNA fractions were fragmented into small pieces using divalent cations under elevated temperature. Then the cDNA libraries were created using the mRNA-Seq sample preparation kit (Illumina, San Diego, CA, USA) following the protocol. The library was paired-end sequenced (PE150) on an Illumina Novaseq™ 6000 (LC Bio Technology CO., Ltd. Hangzhou, China) with 300 bp ( $\pm 50$  bp) following the vendor's recommended protocol.

We aligned reads of all samples to the *Tenebrio molitor* reference genome (<https://www.ncbi.nlm.nih.gov/data-hub/genome/?taxon=7067>) using an HISAT2 (<https://daehwankimlab.github.io/hisat2/>, version: hisat2-2.2.1) package, which initially removed a portion of the reads based on quality information accompanying each read and then mapped the reads to the reference genome. The mapped reads of each sample were assembled using StringTie (<http://ccb.jhu.edu/software/stringtie/>, version: stringtie-2.1.6) with default parameters. Then, all transcriptomes from all samples were merged to reconstruct a comprehensive transcriptome using gffcompare software (<http://ccb.jhu.edu/software/stringtie/gffcompare.shtml>, version: gffcompare-0.9.8). Expression level for all the transcripts was estimated by calculating the FPKM (fragment per kilobase of transcript per million mapped reads) value.

## 2.11. Metabolome analysis

Untargeted metabolomic profiling was performed by a Vanquish Flex ultrahigh-performance liquid chromatography system (Thermo Fisher Scientific, Bremen, Germany) to help build a putative PET degradation pathway. An ACQUITY UPLC T3 column (100 mm  $\times$  2.1 mm, 1.8  $\mu\text{m}$ , Waters, Milford, USA) was used for the reversed phase separation. The samples (100 mg) were first extracted using 1 mL of precooled 50% methanol, vortexed for 60 s, and incubated at room temperature for 10 min. Next, the samples were placed at  $-20^\circ\text{C}$  overnight to precipitate the proteins. After centrifugation (4000 g, 20 min), the cleared supernatant was transferred to sample vials for LC-MS analysis. The mobile phase consisted of solvent A (0.1% formic acid) and solvent B (acetonitrile containing 0.10% formic acid). Gradient elution conducted with the flow rate was 0.40 mL/min. The elution conditions were set as: 0–0.5 min, 5% B; 0.5–7 min, 5% to 100% B; 7–8 min, 100% B; 8–8.1 min, 100% to 5% B; and 8.1–10 min, 5% B.

The generated raw data was preprocessed by the XCMS, CAMERA, and metaX toolbox implemented with the R software. The metabolites were searched in the online database of KEGG (<http://www.genome.jp/kegg/>) and HMDB (<http://www.hmdb.ca/>). During the data analysis, metabolic features detected at least 50% of QC samples and 80% biological samples were retained. In the normalized data matrix, variables with a relative standard deviation > 30% of QC samples were removed.

### 3. Results and discussion

#### 3.1. Confirmation of PET biodegradation using $\delta^{13}\text{C}$ signature

The results of biodegradation of commercial PET MPs have been partially published in a previous companion paper [38] (Fig. S2). Biodegradation of PET in *T. molitor* larvae (500 individuals,  $n = 3$ ) was conducted using commercial PET MPs ( $M_n$  18.59,  $M_w$  29.43 and  $M_z$  39.58 kDa) (Fig. S3). The larvae consumed  $33.86 \pm 0.54$  g PET over 36 days with an average specific consumption rate of 203.00 mg PET/100 larvae/d and a specific removal rate of 152.00 mg/100 larvae/d (Table S1). The survival rate of larvae fed with PET agar gel was slightly higher than that of unfed larvae (Fig. S2a), indicating PET agar gel provided an energy source to the larvae, similar to previous observations when PS, LDPE, PP, PUR, and PLA were fed to mealworms [16,31,36].

PET can be dissolved in 1,1,1,3,3-hexafluoroisopropanol (HFIP). During the test, water soluble, ethanol extracted, and HFIP extracted fractions in the frass of PET-fed larvae were determined (Fig. S2b and Table S2). The residual PET content in the egested frass was estimated using the content of HFIP extracted fractions. The HFIP extractable fraction (% w/w) decreased gradually over the 36-day test period. Mass balance of the ingested PET was calculated as an average 73.28% mass reduction in ingested PET over 36 days (Fig. S2c). The water-soluble fraction contained hydrophilic, digested organic substances, and salts, a portion of which was gradually increased from  $22.94\% \pm 2.13\%$  on day 4 to  $26.36\% \pm 2.12\%$  on day 36. The ethanol-extracted fraction reflected lipophilic substances and accounted for 2.88% to 3.99% of the frass. The residual solid content increased gradually from 33.26% on day 4 to 60.12% on day 36. After extraction with HFIP, the residual solid in the frass included residual enzymes, microorganisms, insoluble metabolized components, and inorganic residues. The results indicated that significant soluble intermediates (>25%) accumulated in the excrement.

As biodegradation leads to the enrichment of heavy natural isotopologues in the non-degraded residual fraction [49,50], in this study,

stable carbon isotope ( $\delta^{13}\text{C}$ ) analysis confirmed that there was significant enrichment of  $^{13}\text{C}$  in residual PET extracted from the frass. The results indicated that in the residual PET polymers,  $\delta^{13}\text{C}$  value increased from  $-27.50\% \pm 0.18\%$  of virgin PET to  $-26.05\% \pm 0.16\%$  ( $p < 0.001$ ) (Fig. 1a). This analysis confirmed biodegradation of PET polymers in larval gut because  $^{12}\text{C}$  was preferentially metabolized by the host and gut microbes during PET biodegradation, thus increasing the  $\delta^{13}\text{C}$  fraction.

The observed PET degradation rate and efficiency in the larvae is much higher than any reported results from microbial in vitro degradation or from degradation in the environment (Table S3). For example, the highest bacterial PET reduction reported was 75% in 75 days by the PET-degrading bacterium *Ideonella sakaiensis* 201-F6 with low-crystallinity PET (1.90%) [51]. On day 4 and day 36, the removal rate of high-crystallinity (18.00%) commercial PET by *T. molitor* larvae was 99 times and then 266 times higher than that of bacterial culture (or a respective half-life of 0.39 and 0.15 d versus 38.50 d) (Table S3).

#### 3.2. Effect of antibiotic suppression

Antibiotic suppression on gut microbes in *T. molitor* larvae has been used to study the role of gut microbes in plastic, and to evaluate whether the gut microorganisms contribute to plastic biodegradation [16,35,52]. The tests of this study were performed to investigate whether the host could depolymerize PET under suppression of gut microbes.

After 5 days of antibiotics treatment, only a few CFUs (about  $26 \times 10^0$ ) were found in the plated samples of the antibiotic treatment group compared to the high CEUs ( $3.24 \pm 0.54 \times 10^4$ ) in the non-treatment control, indicating that the gut microbes were severely depressed or inhibited to an extremely low level (Fig. S4). The larvae in the antibiotic treatment groups were then continuously fed with PET agar gel containing antibiotics for 15 days. No further CFU was found in the gut suspension. GPC analyses showed that PET depolymerization continued and that the reduction of  $M_n$ ,  $M_w$ , and  $M_z$  in the antibiotic treatment group was similar to the levels of the non-antibiotic treatment group without significant difference ( $p > 0.05$ ) (Fig. 1b). This indicated that the larvae performed PET depolymerization independent of gut microbes, i.e., by the host itself. This observation was different from those during biodegradation of PS [5,28,32], LDPE [32,53], PVC [16], and PP [35] by *T. molitor* larvae, i.e., depolymerization of PS, PVC, and PP was severely inhibited or nearly stopped, and depolymerization of LDPE changed pattern. This observation also indicated that the *T. molitor* host has stronger ability to depolymerize/biodegrade PET than other

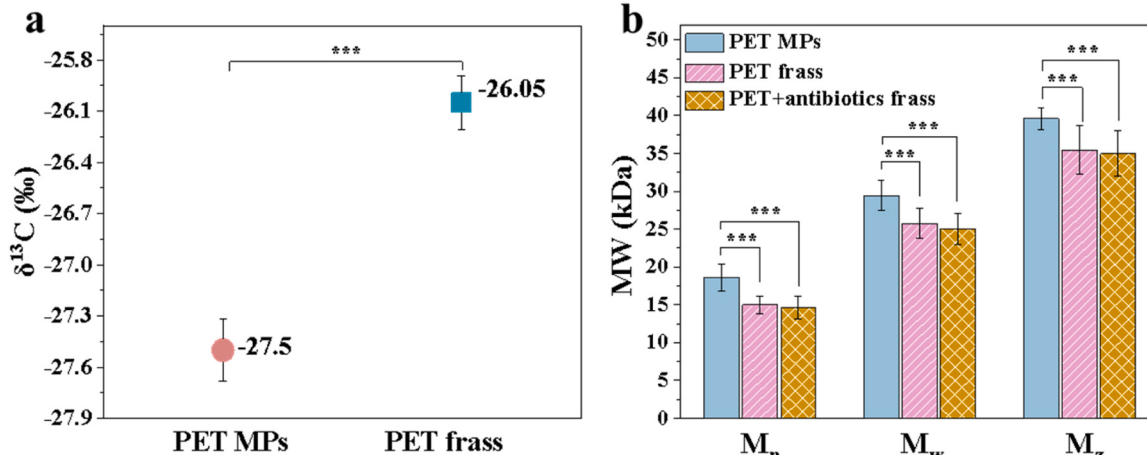


**Fig. 1.** (a) Confirmation of biodegradation of PET with  $\delta^{13}\text{C}$  stable isotope signature of residual PET versus virgin PET MPs. The precision of  $\delta^{13}\text{C}$  measurement was  $\pm 0.20\%$ . (b) Effect of antibiotic suppression by a mixture of the five antibiotics on depolymerization of commercial PET polymers by *T. molitor* larvae by comparison of  $M_w$ ,  $M_n$ , and  $M_z$  of virgin PET versus the residual polymers frass from the larvae fed with PET MPs in the absence and presence of antibiotics ( $n = 3$  samples/group) (Student's t tests, \* :  $p < 0.05$ , \*\* :  $p < 0.01$ , \*\*\* :  $p < 0.001$ , ns: not significantly).

plastics under antibiotic suppression.

### 3.3. Effect of MW on PET degradation

The effect of polymer MW or polymer size on PET biodegradation was investigated by feeding the three high purity PET MPs with  $M_w$  of 1.10, 27.10, and 63.50 kDa in agar gels ( $150.00 \pm 2.00$  mg) versus a normal diet of WB for 16 days ( $n = 3$  groups, individuals = 60). PET<sub>1100</sub> represented low-MW polymers, PET<sub>27100</sub> fit the average MW range of commercial PET as medium-MW polymers, while PET<sub>63500</sub> belonged to high-MW PET group that contributes only a small (e.g., < 2%) portion in commercial PET products. The *T. molitor* larvae consumed all PET MPs.

The weight of the larvae was increased by  $52.10\% \pm 6.10\%$  in WB-fed groups because WB provides abundant nutrients that supported larval development and allowed them to complete their life cycle. Compared to bran, PET lacks essential growth nutrients like proteins, vitamins, minerals, etc., and thus the weight increased less in larvae fed PET as their major food source. The increase in average weight of the PET<sub>27100</sub> fed larvae ( $17.66\% \pm 3.50\%$ ) was similar to those fed PET<sub>63500</sub> ( $17.59\% \pm 2.80\%$ ), and slightly higher than that of PET<sub>1100</sub>-fed groups ( $8.05\% \pm 2.10\%$ ) (Table S4). The lower weight change observed in the PET<sub>1100</sub>-fed larvae could also be attributed to the higher SR in the PET<sub>1100</sub>-fed group ( $69.44\% \pm 2.50\%$ ). For the same amount of diet, more larvae survived in the PET<sub>1100</sub> group than in the PET<sub>27100</sub>- and PET<sub>63500</sub>-fed

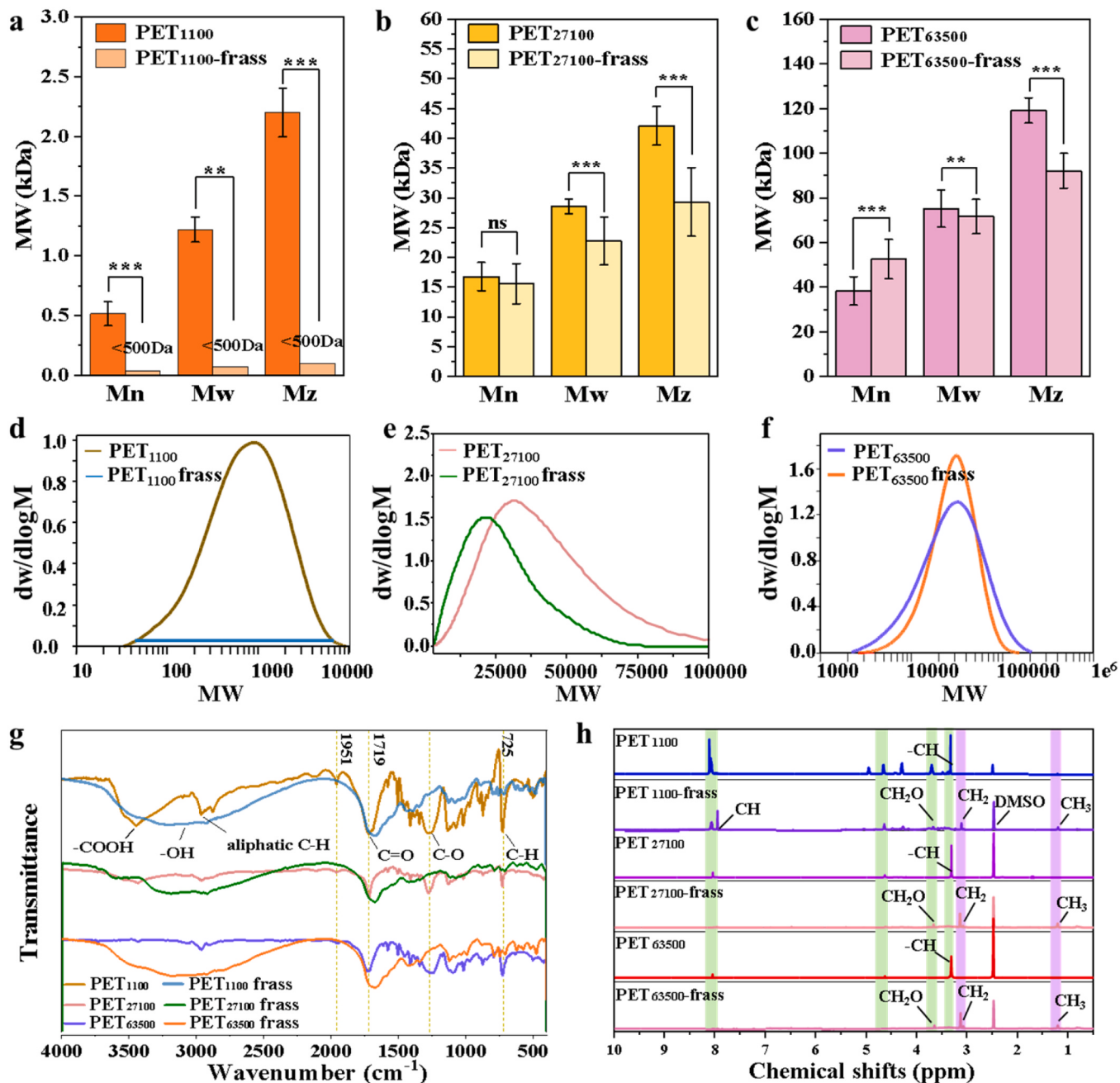


**Fig. 2.** Characterization of biodegradation of three high purity PET polymers by *T. molitor* larvae. Changes in  $M_w$ ,  $M_n$ , and  $M_z$  of three high purity PET MPs PET<sub>1100</sub> (a), PET<sub>27100</sub> (b), and PET<sub>63500</sub> (c) before and after biodegradation by the *T. molitor* larvae (Student's t tests, \* :  $p < 0.05$ , \*\* :  $p < 0.01$ , \*\*\* :  $p < 0.001$ , ns: not significantly). All measurements were conducted in triplicate ( $n = 3$  samples/group); Distributions of MW of PET feedstock PET<sub>1100</sub> (d), PET<sub>27100</sub> (e), and PET<sub>63500</sub> (f) before and after biodegradation by the *T. molitor* larvae; Comparison of FT-IR spectra (g) and <sup>1</sup>H NMR spectra (h) of residual PET polymers in the frass fed with respective PET<sub>1100</sub>, PET<sub>27100</sub>, and PET<sub>63500</sub> versus raw PET polymers.

groups, which resulted in less diet digested per larva, and thus less weight gained.

The residual PET content in the frass was  $4.27\% \pm 0.75\%$ ,  $14.05\% \pm 1.20\%$ , and  $26.02\% \pm 2.01\%$  (w/w) for the larvae fed with PET<sub>1100</sub>, PET<sub>27100</sub>, and PET<sub>63500</sub>, respectively, suggesting that the respective PET mass reduction was at least 95.7%, 86.0%, and 74.0% (Table S4) and that biodegradability of PET did decline as polymer MW increased. PET<sub>27100</sub> represents the MW of most commercial PET and polyester products with MW ranging from 8 to 31 kDa [2]. For high MW, the mass reduction of PET<sub>63500</sub> was still much greater than mass reduction (usually less than 70%) reported for other major plastics (PS, PE, PP and PVC) tested with *T. molitor* larvae [16,31–33,36].

The GPC analysis confirmed that depolymerization degree was impacted by MW. The MW of residual PET from frass fed with PET<sub>1100</sub> was below the detection limit ( $\sim 0.535$  kDa in this study) (Fig. 2d). This could be attributed to the rapid biodegradation of PET<sub>1100</sub> and the PET residue with low MW in the frass. This implies that the consumed PET<sub>1100</sub> was almost completely degraded. M<sub>n</sub>, M<sub>w</sub>, and M<sub>z</sub> of PET<sub>27100</sub> were reduced by 44.23%, 21.83%, and 22.68%, respectively. However, for PET<sub>63500</sub>, M<sub>n</sub> was increased by 37.33% ( $p < 0.001$ ), and M<sub>w</sub> and M<sub>z</sub> were decreased by 4.71% ( $p < 0.01$ ) and 22.86%, respectively ( $p < 0.001$ ). The results demonstrated that PET<sub>1100</sub> and PET<sub>27100</sub> were degraded via BD, while PET<sub>63500</sub> was degraded via LD (Fig. 2a, b, and c). BD pattern generally exhibited a decrease in all MW parameters of the plastic polymer, as well as a shift of MWD towards lower molecular weight (Fig. 2e), indicating a relatively rapid biodegradation of plastics. LD pattern indicated a selective breakdown of polymers of low MW, or an inability to scissor long molecular chains. For PET<sub>63500</sub>, short chain polymers were broken but longer chain polymers also reduced during depolymerization, resulting in narrower MWD after depolymerization (Fig. 2f). This explained the increase in M<sub>n</sub> and decrease in M<sub>z</sub> after degradation of PET<sub>63500</sub>. The different depolymerization patterns implied that lower MW PET was depolymerized more effectively than higher-MW. Based on observations of the MWD of the extracted polymers from the PET-fed frass, the MWD of medium-MW shifted towards the left side of lower MW and the high-MW polymer became narrower compared to the virgin PET. This suggests an overall decrease in MW after PET polymers passed through the larval intestinal tract, although the removal rate of high MW polymers was lower compared to smaller MW polymers (Fig. 2d, e and f).

According to the X-Ray Diffraction crystallinity analyses, the crystallinity degree of PET<sub>1100</sub>, PET<sub>27100</sub>, and PET<sub>63500</sub> were  $53.66\% \pm 3.31\%$ ,  $33.43\% \pm 3.01\%$ , and  $4.25\% \pm 1.64\%$ , respectively. As reported previously, both MW and crystallinity degree impacts enzymatic degradation [54]. Amorphous PET chains were more susceptible to microbial attacks than crystalline regions [12]. The results of this study indicated that MW had a higher negative impact on depolymerization/degradation of PET polymers than crystallinity degree during PET biodegradation by *T. molitor*. Similar results were observed in the previous study of PE degradation by *T. molitor* larvae, i.e., the factors affecting PE biodegradation extent was in the order of M<sub>n</sub> > M<sub>z</sub> > M<sub>w</sub> > PE type > crystallinity degree [33]. Due to the limited availability of PET samples, we could not test PET with both high MW and crystallinity degree, although we hypothesized that it would be more persistent to biodegradation.

FTIR analysis further indicated that the three PET MPs were oxidized in the intestinal tract (Fig. 2g). The FTIR spectra of the three PET MPs showed that the peak at  $1951\text{ cm}^{-1}$  (aromatic summation band) disappeared and bands around  $725\text{ cm}^{-1}$  (C–H) and  $1260\text{ cm}^{-1}$  (C–O stretching from the ether aromatic group) decreased. In contrast, the intensity of oxidized groups increased. Higher intensities were induced and there was a shift of oxidized C=O functional groups from the band of  $1719\text{ cm}^{-1}$  to  $1670\text{ cm}^{-1}$ . The formation of a hydrophilic (hydroxyl) functional group around  $3500$  to  $3250\text{ cm}^{-1}$  suggests an increase in hydrophilicity of the polymers after PET biodegradation [55]. Also, <sup>1</sup>H NMR analysis indicated that the PET residue in frass underwent surface

chemical and structural changes (Fig. 2h). Two peaks located around  $\delta$   $8.1$  ad  $\delta$   $4.7$  ppm of virgin PET polymers corresponded to four protons from the terephthalate ring and the oxyethylene units in the main chain, respectively [56]. The <sup>1</sup>H NMR spectra of residual PET from the frass showed new singlets related to oxidation, i.e., new peaks were detected in chemical shift regions associated with methylene protons ( $-\text{CH}_2\text{O}$ ) and hydroxyl ( $-\text{OH}$ ) groups, indicating obvious evidence of transformations and modifications of PET molecular structure due to biodegradation.

### 3.4. Intestinal microbiome

16 S rRNA gene amplicons were performed to evaluate the gut microbial community responses to the three high purity PET MPs (M<sub>w</sub> 1.10, 27.10, and 63.50 kDa). The results suggested that feeding PET polymers shifted the gut microbial community structure of larvae remarkably (Fig. S6a and b), resulting in reduced gut community richness (Fig. S5a) and diversity (Fig. S5b-d) when compared to the WB-fed larvae (SI R1). The Sankey diagram (Fig. S7a) indicated that Firmicutes and Proteobacteria, two of the common phyla containing plastic degraders [57,58], were predominant in all groups but varied with different proportions. The abundance of Firmicutes was 21.65%, 81.07%, 50.39%, and 71.82% in the control-fed, PET<sub>1100</sub>-fed, PET<sub>27100</sub>-fed, and PET<sub>63500</sub>-fed groups, respectively. Proteobacteria comprised of 55.36%, 10.94%, 15.22%, 14.43% of the phyla in the control-fed, PET<sub>1100</sub>-fed, PET<sub>27100</sub>-fed, and PET<sub>63500</sub>-fed groups, respectively. To date, reported PET degrading bacteria were found in the phylum of Firmicutes (e.g., *Bacillus gottheilii*, *B. cereus*, *B. muralis*) and Proteobacteria (*Ideonella sakaiensis* 201-F6, *Serratia proteamaculans*, *Vibrio* sp.) [51,59]. Firmicutes was the most dominant phylum in the PET-fed groups, whereas Proteobacteria was the most dominant in the control. The results indicated that the gut microbiota of *T. molitor* larvae shifted towards new structures beneficial to PET degradation.

At the genera level (Figs. S6c and S7a), four ASVs including *Cronobacter* sp. (20.16%), *Lactococcus* sp. (13.07%), *Spiroplasma* sp. (12.16%), and unclassified Enterobacteriaceae (10.29%) were the dominant genera in the control group. However, in PETs-fed groups, an ASV of *Lachnotalea* sp., which was not reported in previous studies for PS, LDPE, and PP degradation in *T. molitor* larvae, exhibited the highest abundance, and comprised of 73.53%, 37.18%, and 62.66% of the genera in PET<sub>1100</sub>-fed, PET<sub>27100</sub>-fed, and PET<sub>63500</sub>-fed groups, respectively. Although *Lachnotalea* sp. was found as a potential natural organic polymer-degrader isolated from lignin-enriched microflora [60], the PET-degrading capacity should be further examined. Notably, *Sebaldella* sp., which is related to nitrogen fixation [61] and was not detected in the WB-fed larvae, was a predominant species in the PET fed groups, particularly in the medium-MW PET. *Enterococcus* sp. was found to contribute to PS degradation in *T. molitor* and *G. mellonella*, as reported previously [24,62]. A increase in the abundance of *Enterococcus* sp. was observed in PET-fed larvae compared to the control group, which mostly increased in the low and high-MW PET materials (Fig. S6c).

Two steps were conducted to identify the difference between dominant gut bacteria in PET-fed groups versus the control. The linear discriminant analysis of effect size (LEfse) allowed us to ascertain which abundant gut bacterial species increased as a result of the PET diets (Fig. 3a, b, and c). Subsequently, random forest analyses were employed to verify the most important bacterial species for the formation of between-group differences (Fig. S7b, c and d). Our results showed that two (*Sebaldella* sp. and *Enterococcus* sp.), four (*Sebaldella* sp., *Klebsiella* sp., *Enterococcus* sp., and *Pantoea* sp.), and one (*Enterococcus* sp.) genera were markedly differentiated key species associated with the degradation of PET<sub>1100</sub>, PET<sub>27100</sub>, and PET<sub>63500</sub>, respectively. *Enterococcus* sp., reported to be associated with plastic-degrading microbes [21,63], was found to be the top bacteria (abundance > 2%) in the gut microbiome of the larvae fed on the commercial PET MPs [38]. *Sebaldella termitidis* was isolated from the gut content of the termite *Reticulitermes lucifugus* [61],

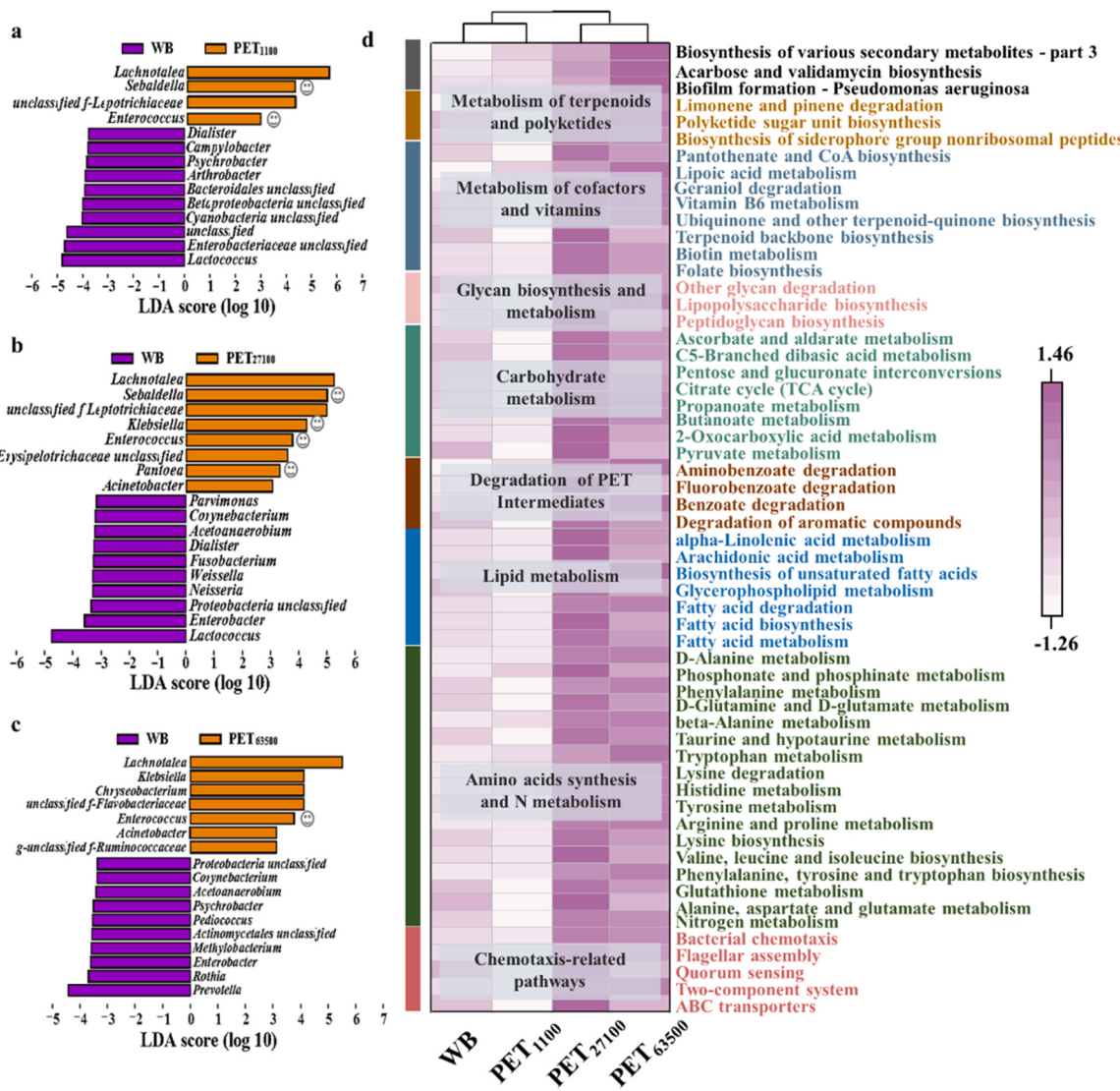


**Fig. 3.** Dominant gut microbial groups and function analyses of *T. molitor* larvae fed with PET diets. The dominant microorganisms based on 16 S rRNA analyses in the samples of PETs-fed larvae versus those the WB fed group (control) by Linear discriminant analysis (LDA) coupled with effect size analysis. (a) PET<sub>1100</sub> vs WB, (b) PET<sub>27100</sub> vs WB, (c) PET<sub>63500</sub> vs WB. Only top ten genus of bacteria in each group are presented. The species marked by the smiley faces were also appeared in the result of random forest analyses, which could be markedly differentiated key species associated with degradation of PET<sub>1100</sub>, PET<sub>27100</sub>, and PET<sub>63500</sub>, respectively; (d) Relative abundances of annotated genes at PathwayDefinition of KEGG hierarchy which are more abundant in the PETs-fed samples in metagenomic sequencing libraries. PET<sub>1100</sub>, PET<sub>27100</sub> and PET<sub>63500</sub> are high purity PET polymer powders with respective MW of 1.10, 27.10 and 63.50 kDa.

and played a role in providing nitrogen to the host. *Pantoea* sp. and *Klebsiella* sp. are associated with both nitrogen fixation and plastic degradation. *Pantoea* sp. was isolated from sugarcane tissues as an endophytic nitrogen-fixing bacterium [64]. *Klebsiella* species were associated with biodegradation of PS [53] and PVC [21], and also nitrogen fixation [65]. Overall, the bacterial species found in the PET-fed group were either reported to be associated with plastic biodegradation or nitrogen-fixation. The gut microbiome for PET degradation could likely be due to ordinal gut microbes digesting lignocellulose in their natural diet [26,48,66].

The emergence of bacteria with nitrogen-fixation abilities during PET degradation was a result of feeding nutrient-poor diets (i.e., PET and agar). Under nitrogen-deficient conditions, insects benefited from symbiotic bacteria capable of fixing gaseous nitrogen to synthesize amino acids [54,65]. This indicated that *T. molitor* larvae quickly adapted to the PET diet by shifting their gut microbial community composition in order to synthesize the required enzymes via nitrogen fixation [54].

### 3.5. Contributions of gut bacteria

Metagenome sequencing was used to investigate the potential contribution of the gut bacteria to PET biodegradation pathways with a focus on genes related to PET degradation and metabolic pathways. Overall, the gene sets involved in the metabolism category of KEGG enrichment was predominant among the three PET-fed samples (Fig. 4a). Genes encoding enzymes related to the degradation of PET and its oligomers as well as enzymes responsible for modifying the PET surface, such as esterase/lipase [67,68] (K14731), carboxylesterase [69, 70] (K02170), and alkane-1 monooxygenase [57] (K00496), were found in the PET-fed groups (Fig. 4b). Esterase/lipase, which was reported as a PET surface-modifying enzyme, can initiate the biodegradation process attack on the ester of PET. Carboxylesterase was reported to be very active toward PET oligomers [70]. Alkane 1-monooxygenase can introduce oxygen to the alkane substrate [57], and could breakdown hydrocarbons by acting on the C–C bonds and transforming them to alcohols. Degradation of PET by alkane 1-monooxygenase has not been

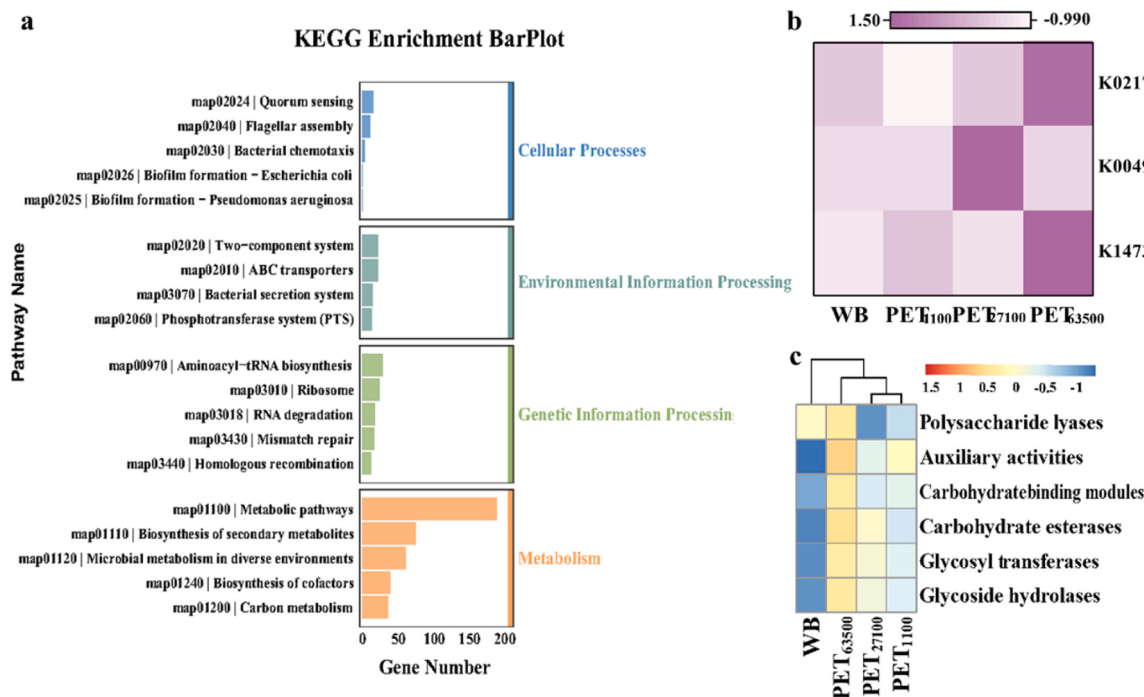


**Fig. 4.** Metagenome sequencing analysis of PET-degrading metabolic functions of the gut microbes in *T. molitor*. (a) Enriched KEGG genes of three PET-fed groups by metagenome sequencing analysis. (b) Heatmap plot of the esterase/lipase (K14731), carboxylesterase (K02170), and alkane-1 monooxygenase encoding-related genes (K00496); (c) Heatmap of CAZy function classification at level 1 of CAZy hierarchy.

reported before, although it was found to be enriched in aerobic microbiome attached to PET [71]. The CAZy (carbohydrate-active enzymes) database provides classification of and information on enzymes involved in the synthesis, metabolism, and transport of carbohydrate compounds. Many lignocellulose- and plastic-degrading enzymes were under the category of CAZymes. The results showed that the enzymes classified as carbohydrate esterase were more abundant in PET samples than those in the control sample (Fig. 4c). This also suggested that hydrolase-related enzymes in gut bacteria could contribute to the surface modifying and metabolism of intermediate products during PET degradation, especially for PET with higher MW. Given the results of Fig. 4, unlike non-hydrolyzable polymer such as PS and PE, hydrolase-related enzymes in gut bacteria exerted a crucial role during PET biodegradation. During this process, enzymes involved in oxidation could contribute to hydroxylation of C–C bonds as an auxiliary support.

On the other hand, Jahanshahi et al. [72] analyzed genes in samples from plastic-contaminated environments and found that glycoside hydrolase, glycosyltransferase, auxiliary activities, and carbohydrate-binding modules were all related to plastizymes. In this study, genes encoding these families in the CAZy database were all more abundant in the three PET-fed samples than in the WB fed samples, indicating a powerful source of PET-degradation enzymes of these families. The contribution of these enzymes to PET degradation might be similar to the role they play in the degradation of natural substances. For example, Lou et al. [73] found that genes encoding the CAZymes were closely related to lignocellulose degradation.

KEGG is a knowledge base for systematic analysis of gene functions, linking genomic information with higher order functional information. In PET-fed and control groups, a total of 149 KEGG pathways were annotated (Data S1). Here, the functional information related to PET metabolism is displayed at the level of KEGG Pathway Definition by heatmap (Fig. 3d). Overall, PET<sub>1100</sub>- and WB-fed samples clustered together, suggesting these pathways did not function during the degradation of PET<sub>1100</sub>. Similar to the abundance of PET-degradation related enzymes, abundance of KEGG enrichment associated with PET

metabolism were also at a low level in PET<sub>1100</sub>. This was attributed to the easier degradability of PET<sub>1100</sub> than PET<sub>27100</sub> and PET<sub>63500</sub>. This result indicated that the host is able to complete the degradation of PET<sub>1100</sub>, resulting in less contribution of the gut bacteria during low MW of PET degradation.

Specifically, the results showed the presence of the transport systems for degradation of PET fragments in all of the PET-fed gut microbiota. The differential genes between PET<sub>27100</sub> and PET<sub>63500</sub>-fed groups and the control group were highly enriched in the pathway of ATP binding cassettes (ABC) transporters. In the PET<sub>1100</sub>-fed group, the KEGG pathway of ABC transporters was also noted, although the abundance of transportation appeared relatively weak. Similar observations were made for a marine bacterium, *Bacillus species AIW2*, which exhibited upregulation of ABC transporter genes during PET degradation [4]. Moreover, the significantly high enrichment of synthesis of various secondary metabolites observed in PET-fed groups indicated that the gut microbiota served as the secondary PET degrader because *T. molitor* larvae can degrade PET under antibiotic suppression. Because macromolecule plastics (polymer chains > 50 carbon atoms) cannot transport through cell membranes [74], the PET polymer chains have to be depolymerized or hydrolyzed outside the bacterial cells. Once the molecular size of the depolymerized products were reduced or degraded to 10–50 carbon atoms, they could penetrate bacterial cells through transport proteins and be further metabolized [70].

Furthermore, various functions related to chemotaxis (such as two-component systems, quorum sensing, flagellar assembly, and bacterial chemotaxis), were highly enriched in gut bacteria fed with medium and high MW PET (i.e., PET<sub>27100</sub> and PET<sub>63500</sub>) but appeared slightly weak in the PET<sub>1100</sub> group (Fig. 3d). Bacterial chemotaxis towards aromatic compounds has been frequently observed, such as benzoate, benzene derivatives, 4-hydroxybenzoate, and protocatechuate [75], which can be used by bacteria as a source for carbon and energy. Different genes in pathways possibly related to PET degradation were abundant in the three PET-fed samples for the degradation of aromatic compounds (e.g., benzoate, amino benzoate, fluorobenzoate) (Fig. 3d), suggesting that the

gut microbes contributed to degradation of PET metabolites. Thus, as discussed above, the gut bacteria had chemotaxis towards the PET metabolic intermediates under non-preferential dietary conditions during PET degradation.

The results indicated that the gut microbiota showed chemotaxis towards aromatic compounds (e.g., benzoate, amino benzoate, and fluorobenzoate) as frequently observed [57], and served as the secondary PET degrader. After the PET polymer chains are depolymerized or hydrolyzed outside the bacterial cells with the molecular size of the depolymerized products reduced or degraded to 10–50 carbon atoms [57], they could penetrate bacterial cells through transport proteins and be further metabolized [70]. The low abundance of transportation and chemotaxis-related genes in PET<sub>1100</sub> could be due to the fact that the larvae possessed higher digestive ability toward low MW polymers and thus the gut microbes contributed less to the biodegradation of low MW PET than to the biodegradation of medium and high MW PET.

Genes involved in lipid metabolism were also abundant in PET<sub>27100</sub>- and PET<sub>63500</sub>-fed groups (Fig. 3d). Therein, FA is one of the main energy sources of the body and FA derivatives are important components of insect epidermis. Long chain FAs are the precursors of sphingolipids and glycolides, which are essential components of the cell membrane structure and are involved in a variety of cellular biological processes [76]. As a result, FA biosynthesis-related pathways contribute to many

cellular biological processes and energy reserves during PET degradation in the larvae. Gut microbes also provide bioemulsifying factors to accelerate plastic degradation [53]. The genes enriched in pathways of FA metabolism and degradation implied that the degradation of FA from PET could be performed by gut bacteria. The formation of carboxylic acid products are analogous to FAs, which can be catabolized by bacteria into the tricarboxylic cycle [11]. This indicated energy reserves and FA degradation from PET could be performed by gut bacteria [11,53,76].

Besides PET degradation, pathways of nitrogen metabolism and biosynthesis of nutrients (cofactors and vitamins) were abundant in the PET<sub>27100</sub>- and PET<sub>63500</sub>-fed samples compared with the control group. Under nutritional deficiency, many insects harbor symbiotic bacteria that synthesize essential amino acids and/or vitamins for their hosts [77]. In this study, *T. molitor* larvae modified their gut microbiota to form a new community that could provide the source of nitrogen via nitrogen fixation in the larvae fed PET. However, compared with the high protein content in normal feed (e.g., WB), nitrogen provided by N-fixing bacteria was limited, and supplementation of nutrition-rich diets would be required for long-term survival because gut nitrogen-fixing bacteria could only provide the equivalent protein of 8.60 to 23.00 µg per day for each larva fed plastic only, e.g., PS foam [65].

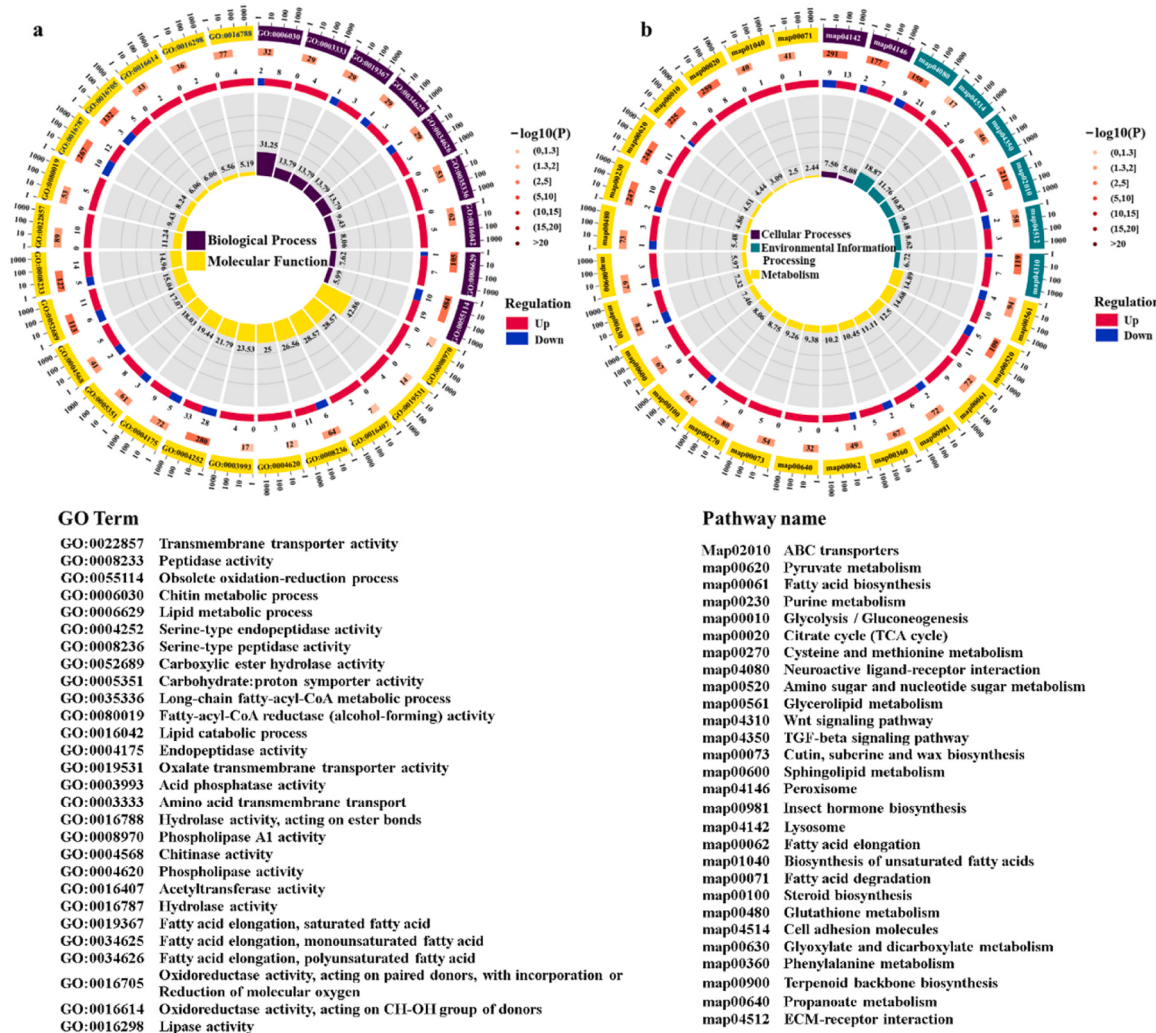


**Fig. 5.** Transcriptomic analysis of PET-degrading metabolic functions of the host *T. molitor* larvae ( $n = 3$  sample/group). (a) LoopCircos of GO enrichment of differential upregulated genes between the PETs-fed samples and the control sample ( $p < 0.05$ ). (b) LoopCircos of KEGG pathways enrichment of differential upregulated genes between the PETs-fed samples and the control sample ( $p < 0.05$ ).

### 3.6. The transcriptome profile of *T. molitor* larvae during PET degradation

As antibiotic suppression tests demonstrated that PET depolymerization could also happen under inhabitation of intestinal microorganisms, transcriptome analysis was employed to evaluate the role of the larvae host in PET biodegradation by examining the digestive gene expression of *T. molitor* larvae. Principal component analysis (Fig. S8a) and Pearson correlation analyses (Fig. S8b) showed that the three PET-fed groups clustered together but far away from control samples. The results implied that the metabolism of the host on low, medium, and high MW PET exhibited similarity regardless of the MW of PET. Compared with the analyses result in Fig. S6a, the host was less sensitive to different MW of PET than its gut microbes. Similar to gut microbes, the most upregulated genes which related to the KEGG pathway of ABC transporters suggested that nutrient-deficient food could lead to increased nutrient acquisition capacity in the larvae [78] (Fig. 5b).

The transcriptome analysis indicated that the pathways for hydrolysis were induced after PET feeding. This provides a framework and set of concepts for describing the functions of gene products from all organisms. For the three PET-fed groups, high Gene Ontology (GO) enrichments were observed in carboxylic ester hydrolase activity (GO:0016788), hydrolase activity acting on ester bonds (GO:0016788), hydrolase activity (GO:0016787), peptidase activity (GO:0008233), endopeptidase activity (GO:0004175), serine-type endopeptidase activity (GO:0004252), lipase activity (GO:0016298), cellulase (GO:0008810, GO:0030245), phospholipase activity, and serine-type peptidase activity (GO:0008236) (Fig. 5a), indicating that many gene families were activated for PET hydrolysis and metabolism in *T. molitor*. The GOs were probably responsible for enhancing the production of long-chain FAs, long-chain alcohols, or long-chain C-C or C-N linked carbonyls or carbonyls from PET. Particularly, overexpression of carboxylic ester hydrolases was observed, including that of lipase (EC:3.1.1.13) and carboxylesterase (EC:3.1.1.1, EC:3.1.1.7, EC:3.1.1.59) (Data S2), which are typical enzymes that act on ester bonds. This supports the possibility of PET hydrolysis in by the host. In this study, many genes encoding for carboxylesterases, which can cleave ester bonds (short-chain acyl ester) and facilitate the surface modification of PET [79], were found extensively in the PET-fed larvae. Although FPKM of lipase encoding genes was low, it was clearly activated in the PET-fed samples, compared with the control samples.

Oxidases were also overexpressed in the three PET-fed groups. Enzymes related to drug metabolisms (cytochrome P450 (CYP450) [45,76] and glutathione S-transferases) and laccase were activated in the gut tissue of larvae (Data S2). CYP450s belong to a superfamily of monooxygenases, which can catalyze diverse reactions, such as C-H hydroxylation, C=C double bond epoxidation, heteroatom oxygenation, and C-C bond cleavage in complex organic molecules [45]. A recent study conceived a CYP450-driven cascade enzymatic PE degrading pathway in synthetic bacteria to degrade PE [76]. Glutathione S-transferases can further transform intermediates by catalyzing the conjugation of the tripeptide glutathione to electrophilic centers of non-polar compounds, making them more water soluble [80]. Laccase is a widely reported oxidative enzyme known to decompose PE and aromatic compounds [67]. These findings suggested that the upregulated enzymes supported the observation of PET degradation by the host. Further research is needed to characterize roles of individual enzymes.

Similar to the genes of the gut bacteria, lipid metabolism related genes (FA degradation, FA biosynthesis, FA elongation, steroid biosynthesis, sphingolipid metabolism, glycerolipid metabolism, and cutin, suberine and wax biosynthesis) expanded in PET-fed groups (Fig. 5b), which is consistent with the response of other insects toward dietary restrictions [45,81]. Besides energy reservation and the assimilation of biodegraded intermediates into biomass, the upregulation of lipid metabolism related genes could also partially be due to the oxidative stress response to PET MPs ingested by the larvae host (SI R2, Fig. S9)

[45,82]. LeMoine et al. [45] surmised that an important metabolic remodeling associated with lipid homeostasis happened when *G. mellonella* larvae were fed with LDPE. Thus, the change of lipid homeostasis could be due to multiple factors including assimilation, stress response, and other bioreactions.

### 3.7. Metabolome analysis

Untargeted metabolomics was performed to identify key metabolites during PET biodegradation in order to understand PET metabolic pathways. In the differential metabolite heatmap of the PET-fed groups versus agar-fed control group (Fig. S10), typical PET-degrading intermediates were abundant in the PET-fed samples, such as benzoic acid, protocatechuic acid, and catechol [55]. Compared with the control, 45, 45, and 65 identified metabolites were differentially accumulated in the three PET groups (fold change (FC)  $\geq 2.00$ ,  $p < 0.05$ ). According to the KEGG mapping results, the significantly upregulated differential metabolites identified were classified into six specific MS2 classes: benzoids, lipids, and lipid-like molecules, organic acids and derivatives, organic nitrogen compounds, organic oxygen compounds, and organoheterocyclic compounds (Fig. S11). The metabolome results supported the analyses through the host and gut microbiomes. In detail, the upregulated nitrogen compounds in PETs-fed larvae further supported nitrogen fixation mechanism for insect survive on PET with low nutrient content (Fig. S11), as has been validated at the microbiome and metagenome levels. The most enriched KEGG in metabolic expression in all the three PETs-fed samples was glycerophospholipid metabolism (Fig. 6 a, b, c), which was closely linked to the maintenance of optimal physical properties and functions of cell membranes, and it also correlates with normal mitochondrial functions in the gut microbiome. It could be a stress response caused by microplastics. This is consistent with the above discussion about lipid homeostasis in host transcriptome, demonstrating consuming of PET triggered oxidative stress response in the host during the degradation of PET. Many of the significantly accumulated metabolites were enriched in the KEGG pathway of aromatic/polycyclic-aromatic hydrocarbon degradation, benzoate degradation, ethylbenzene degradation, and ether lipid metabolism (Fig. 6 a, b, and c), also supporting production of intermediates from PET degradation as analyses by microbiome and host transcriptome. In detail, based on the result of microbiome and transcriptome analyses, various hydrolases that typically act on ester bonds supported the PET hydrolysis. This could result in production of hydrolysing products of PET, i.e., bis (2-hydroxy ethyl) terephthalate (BHET), mono (2-hydroxy ethyl) terephthalate (MHET), terephthalic acid, and ethylene glycol. Above metabolome analysis revealed the presence of benzoic acid, protocatechuic acid, and catechol in the PET-fed samples (Fig. S10), which are key products from PET biodegradation. During PET degradation, typical hydrolyzed products of PET (MHET), which was produced by various hydrolases from hosts and gut microbes, could be metabolized into EG and terephthalic acid. Terephthalic acid (TPA) is usually metabolized into protocatechuic acid, which can be further degraded via catechol [1]. Further research is needed to identify the metabolic intermediates in detail via various analytical methods.

Based on the results from this study and the current knowledge, we propose a primary PET degradation pathway in *T. molitor* larvae performed by the host and gut microbes (Graphic Abstract and Fig. 7) and summarized in the following basic steps: (a) the larvae chew PET materials into smaller fragments ( $< 75 \mu\text{m}$ ) and ingest them together with air ( $\text{O}_2$  and  $\text{N}_2$ ) into the foregut; (b) from the foregut to the midgut, PET fragments move and mix with digestive fluid, gut microbes, and extracellular enzymes secreted by the host and microbiota. In the midgut, PET is depolymerized by various hydrolases and oxidases from the host and its gut microbes. Subsequently, multiple enzymes synergistically break down the PET and intermediates, including carboxylesterase, laccase, lipase, oxygenases, CYP 450, phospholipase, and glutathione S-transferase. Previous study indicated the pH of anterior- and medium-midgut

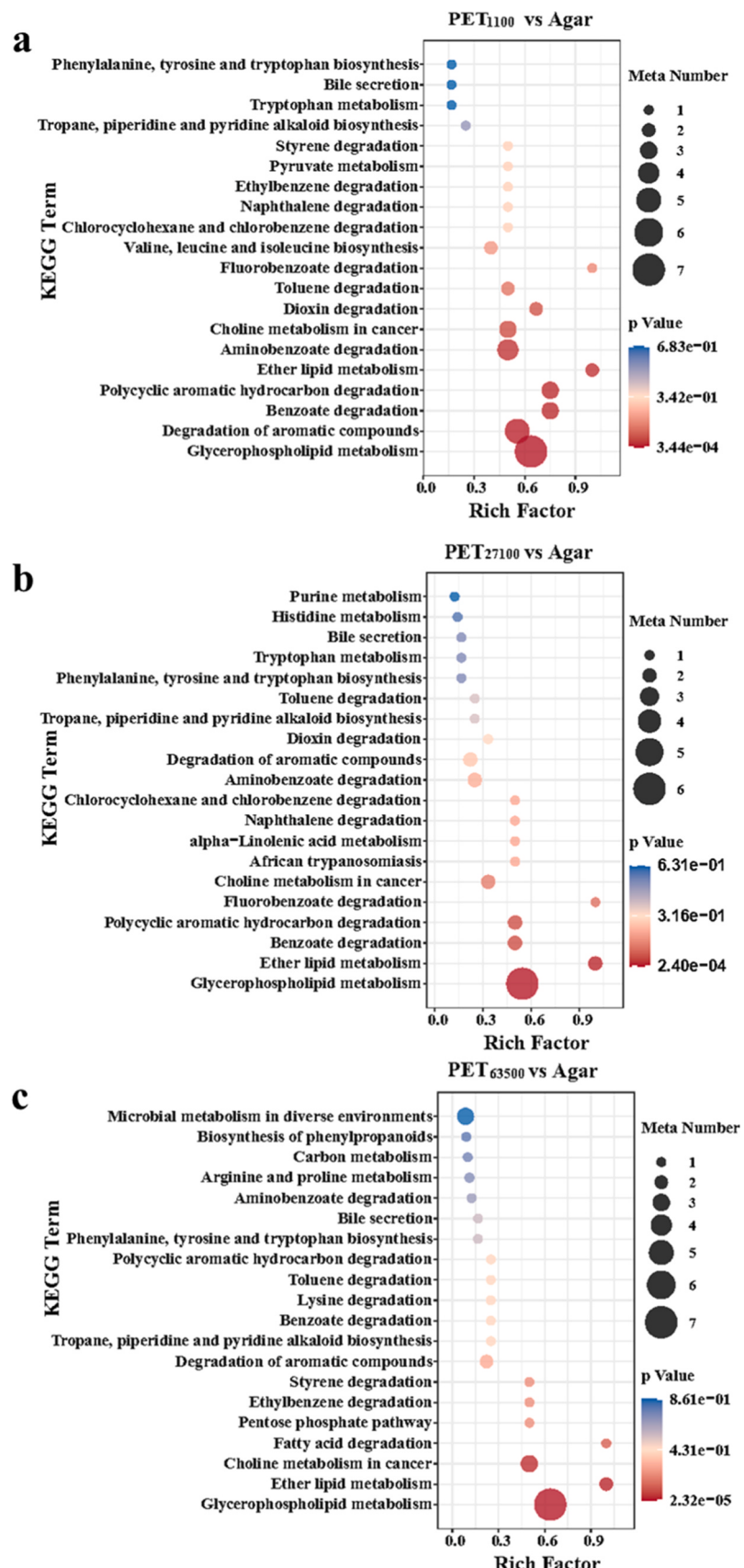


**Fig. 6.** Intestinal metabolic expression in PETs-fed larvae. Scatter plot of KEGG enrichment of differential genes between PET<sub>1100</sub>-fed sample (a), PET<sub>27100</sub>-fed sample (b), and PET<sub>63500</sub>-fed sample (c) compared with the control group

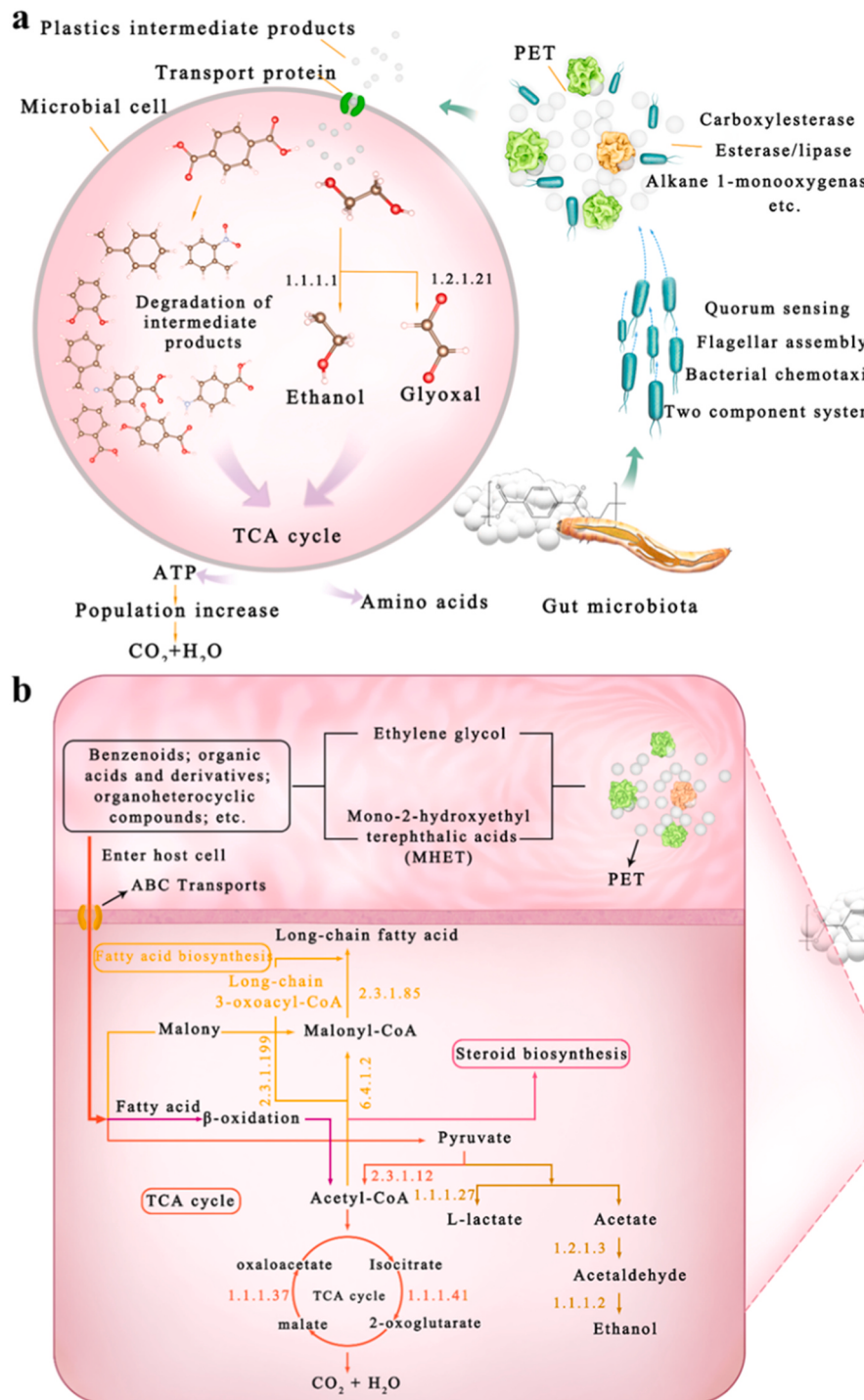


Fig. 7. Putative PET degradation pathway contributed by the gut microbiomes (a) and the host *T. molitor* larvae only (b).

of the larvae was pH 5.60 and progressively increased to 7.90 in the posterior midgut [83]. The pH condition is favorable for PET depolymerization since hydrolysis favors acidic or basic conditions [84]. (c) Enzymes secreted by host and microbiota further degraded the intermediates, thus reducing the size of residual fragments. (d) Transport proteins aid uptake of decomposed products by microbes and host cells for further intracellular metabolism. In the midgut and hindgut, a majority of biodegraded intermediates are mineralized into CO<sub>2</sub> and H<sub>2</sub>O with energy generation by multiple functional microbes and host cells. A fraction of carbons of the intermediates are assimilated into biomass. (e) During PET degradation, O<sub>2</sub> is consumed for oxidative reactions in the

midgut, and nitrogen fixing bacteria convert N<sub>2</sub> to amino acids to supplement N for enzyme synthesis, maintaining PET digestion and life activities.

The observed PET degradation rate and efficiency in the larvae is much higher than any reported results from microbial in vitro degradation or the environment degradation (Table S3). For example, the highest bacterial PET reduction reported was 75% in 75 days by the PET-degrading bacterium *Ideonella sakaiensis* 201-F6 with low-crystallinity PET (1.9%) [51]. On day 4 and day 36, the removal rate of high-crystallinity (18%) commercial PET by *T. molitor* larvae was 99 and then 266 times higher than that of the bacterial culture (or a respective

half-life of 0.39 and 0.15 d versus 38.50 d) (Table S3).

#### 4. Conclusions and future studies

The results of this study indicate that PET polymers with MW ranges of commercial products even up to 63.5 kDa can be biodegraded effectively in *Tenebrio molitor* larvae using analytical evidences (mass reduction, GPC, FTIR, <sup>1</sup>H NMR etc.), and especially.

- a) *T. molitor* larvae biodegrade the hydrolysable polymer PET with a half-life (0.15 to 039 day) that is much less than that of non-hydrolysable polymers such as PS and LDPE;
- b) PET polymer size impacts mass reduction and depolymerization pattern, while the gut microbiome can adapt to a PET diet [28,30];
- c) the host digestive system is capable of degrading PET independent of gut microbes, and the enzymes secreted by the *T. molitor* host plays a key role in PET biodegradation, as observed under antibiotic suppression; and
- d) the gut microbiota contribute significantly to PET biodegradation, and the biodegradation of PET in *T. molitor* should be considered as symbiotic activities between the gut microbes and the host.

In addition, the gut microbiome for PET degradation could be likely due to ordinal gut microbes digesting lignocellulose in their natural diet. Methodically, this study also demonstrated that the increase in  $\delta^{13}\text{C}$  of residual PET polymer can serve as an effective indication to access biodegradation. The results revealed that PET was synergistically biodegraded by host digestive enzymes together with gut microbes, although the host is able to depolymerize PET independent of gut microbes as well.

To date, low-crystallinity and amorphous PET materials have been widely tested to study enzymatic PET degradation [13,51,85]. *T. molitor* is a model insect for research on plastic degradation. We hypothesize that similar mechanisms for PET biodegradation could also be present in the larvae of other darkling beetles such as *Zophobas atratus*, *Tribolium castaneum*, *Plesiophthalmus davidi*, and *Uloma* etc. More research is needed to verify this hypothesis.

#### Funding

The authors gratefully acknowledge the National Natural Science Foundation of China (Grant No. 52170131), National Engineering Research Center for Bioenergy (Harbin Institute of Technology, Grant No. 2021A001), the Open Project of State Key Laboratory of Urban Water Resource and Environment (Harbin Institute of Technology) (Grant No. 2021TS35), and the National Funded Postdoctoral Research Program of China (Certification Number, GZC20232543). Dr. W.-M. Wu appreciates the support by the Woods Institute for Environment at Stanford University (Award 1197667–10-WTAZB).

#### CRediT authorship contribution statement

**Ding Jie:** Writing – review & editing, Validation, Supervision, Methodology, Funding acquisition, Conceptualization. **Chen Cheng-Xin:** Formal analysis, Conceptualization. **He Lei:** Writing – review & editing, Writing – original draft, Validation, Supervision, Methodology, Formal analysis, Conceptualization. **Wu Wei-Min:** Writing – review & editing, Validation, Supervision, Methodology, Conceptualization. **Yang Shanshan:** Writing – review & editing, Validation, Supervision, Methodology, Funding acquisition, Conceptualization. **Pang Ji-Wei:** Methodology, Formal analysis. **Peng Bo-Yu:** Methodology. **Yang Fan:** Formal analysis, Conceptualization. **He Zhi-Li:** Writing – review & editing, Validation. **Ren Nan-Qi:** Conceptualization. **Zhang Yalei:** Methodology, Formal analysis. **Xing De-Feng:** Conceptualization.

#### Declaration of Competing Interest

The authors declare that they have no known competing financial interests or personal relationships that could have appeared to influence the work reported in this paper.

#### Data Availability

Data will be made available on request.

#### Acknowledgements

The authors appreciate Professor Craig S. Criddle, Stanford University, for his support and suggestion during this study. We gratefully acknowledge the support of the Heilongjiang Province Touyan Team, and the help in manuscript preparation by Ms. Andria T. Wu, DePaul University, and Ms. Julia T. Wu, University of Wisconsin, Madison.

#### Supplementary material

The following files are available free of charge.

Additional file:

**Supplementary Material :** Including Methods S1 to S3#; Results S1 to S2#; Figs. S1 to S11#; Tables S1 to S4#.

**Supplementary Data S1.**

**Supplementary Data S2.**

#### Appendix A. Supporting information

Supplementary data associated with this article can be found in the online version at doi:10.1016/j.jhazmat.2024.133446.

#### References

- [1] Farah, S., Kunduru, K.R., Basu, A., Domb, A.J., 2015. Poly(Ethylene terephthalate) based blends, composites and nanocomposites. William Andrew Publishing, Oxford, pp. 143–165. <https://doi.org/10.1016/B978-0-323-31306-3.00008-7>.
- [2] Plastics - the facts 2022. Plastics Europe. (<https://plasticseurope.org/knowledge-hub/plastics-the-facts-2022/>).
- [3] Rahimi R., S., Nikbin, I.M., Allahyari, H., Habibi T., S., 2016. Sustainable approach for recycling waste tire rubber and polyethylene terephthalate (PET) to produce green concrete with resistance against sulfuric acid attack. *J Clean Prod* 126, 166–177. <https://doi.org/10.1016/j.jclepro.2016.03.074>.
- [4] Kumari, A., Bano, N., Bag, S., Chaudhary, D., Jha, B., 2021. Transcriptome-guided insights into plastic degradation by the marine bacterium. *Front Microbiol* 12. <https://doi.org/10.3389/fmicb.2021.751571>.
- [5] Yang, S.-S., Wu, W.-M., Pang, J.-W., He, L., Ding, M.-Q., Li, M.-X., Zhao, Y.-L., Sun, H.-J., Xing, D.-F., Ren, N.-Q., Yang, J., Criddle, C.S., Ding, J., 2023. Bibliometric analysis of publications on biodegradation of plastics: explosively emerging research over 70 years. *J Clean Prod* 428, 139423. <https://doi.org/10.1016/j.jclepro.2023.139423>.
- [6] Müller, R.-J., Kleeberg, I., Deckwer, W.-D., 2001. Biodegradation of polyesters containing aromatic constituents. *J Biotechnol* 86, 87–95. [https://doi.org/10.1016/S0168-1656\(00\)00407-7](https://doi.org/10.1016/S0168-1656(00)00407-7).
- [7] Tournier, V., Duquesne, S., Guillamot, F., Cramail, H., Taton, D., Marty, A., André, I., 2023. Enzymes' power for plastics degradation. *Chem Rev* 123, 5612–5701. <https://doi.org/10.1021/acs.chemrev.2c00644>.
- [8] Kushwaha, A., Goswami, L., Singhvi, M., Kim, B.S., 2023. Biodegradation of poly(ethylene terephthalate): mechanistic insights, advances, and future innovative strategies. *Chem Eng J* 457, 141230. <https://doi.org/10.1016/j.cej.2022.141230>.
- [9] Cai, Z., Li, M., Zhu, Z., Wang, X., Huang, Y., Li, T., Gong, H., Yan, M., 2023. Biological degradation of plastics and microplastics: a recent perspective on associated mechanisms and influencing factors. *Microorganisms* 11, 1661. <https://doi.org/10.3390/microorganisms11071661>.
- [10] Urbanek, A.K., Kosiorowska, K.E., Mirończuk, A.M., 2021. Current knowledge on poly(ethylene terephthalate) degradation by genetically modified microorganisms. *Front Bioeng Biotechnol* 9, 771133. <https://doi.org/10.3389/fbioe.2021.771133>.
- [11] Mohanan, N., Montazer, Z., Sharma, P.K., Levin, D.B., 2020. Microbial and enzymatic degradation of synthetic plastics. *Front Microbiol* 11, 580709. <https://doi.org/10.3389/fmicb.2020.580709>.
- [12] Carr, C.M., Clarke, D.J., Dobson, A.D.W., 2020. Microbial polyethylene terephthalate hydrolases: current and future perspectives. *Front Microbiol* 11, 571265. <https://doi.org/10.3389/fmicb.2020.571265>.
- [13] Brizendine, R.K., Erickson, E., Haugen, S.J., Ramirez, K.J., Mischall, J., Salvachúa, D., Pickford, A.R., Sobkowicz, M.J., McGeehan, J.E., Beckham, G.T., 2022. Particle size reduction of poly(ethylene terephthalate) increases the rate of

- enzymatic depolymerization but does not increase the overall conversion extent. ACS Sustain Chem Eng 10, 9131–9140. <https://doi.org/10.1021/acssuschemeng.2c01961>.
- [14] Bombelli, P., Howe, C., Bertocchini, F., 2017. Polyethylene bio-degradation by caterpillars of the wax moth *Galleria mellonella*. Curr Biol 27, R292–R293. <https://doi.org/10.1016/j.cub.2017.02.060>.
- [15] Kong, H.G., Kim, H.H., Chung, J., Jun, J., Lee, S., Kim, H.-M., Jeon, S., Park, S.G., Bhak, J., Ryu, C.-M., 2019. The *Galleria mellonella* hologenome supports microbiota-independent metabolism of long-chain hydrocarbon beeswax. Cell Rep 26, 2451–2464.e5. <https://doi.org/10.1016/j.celrep.2019.02.018>.
- [16] Peng, B.-Y., Chen, Z., Chen, J., Yu, H., Zhou, X., Criddle, C.S., Wu, W.-M., Zhang, Y., 2020. Biodegradation of polyvinyl chloride (PVC) in *Tenebrio molitor* (Coleoptera: Tenebrionidae) larvae. Environ Int 145, 106106. <https://doi.org/10.1016/j.envint.2020.106106>.
- [17] Woo, S., Song, I., Cha, H.J., 2020. Fast and facile biodegradation of polystyrene by the gut microbial flora of *Plesiophthalmus davidi*s larvae. Appl Environ Microbiol 86, e01361-20. <https://doi.org/10.1128/AEM.01361-20>.
- [18] Kundugal, H., Gangarapu, M., Sarangapani, S., Patchaiyappan, A., Devipriya, S.P., 2021. Role of pretreatment and evidence for the enhanced biodegradation and mineralization of low-density polyethylene films by greater waxworm. Environ Technol 42, 717–730. <https://doi.org/10.1080/09593330.2019.1643925>.
- [19] Zhong, Z., Nong, W., Xie, Y., Hui, J.H.L., Chu, L.M., 2022. Long-term effect of plastic feeding on growth and transcriptomic response of mealworms (*Tenebrio molitor* L.). Chemosphere 287, 132063. <https://doi.org/10.1016/j.chemosphere.2021.132063>.
- [20] Zhang, S., He, Z., Wu, C., Wang, Z., Mai, Y., Hu, R., Zhang, X., Huang, W., Tian, Y., Xia, D., 2022. Complex bilateral interactions determine the fate of polystyrene micro- and nanoplastics and soil protists: implications from a soil amoeba. Environ Sci Technol 56, 4936–4949. <https://doi.org/10.1021/acs.est.1c06178>.
- [21] Zhang, Z., Peng, H., Yang, D., Zhang, G., Zhang, J., Ju, F., 2022. Polyvinyl chloride degradation by a bacterium isolated from the gut of insect larvae. Nat Commun 13, 5360. <https://doi.org/10.1038/s41467-022-32903-y>.
- [22] Sanluis-Verdes, A., Colomer-Vidal, P., Rodriguez-Ventura, F., Bello-Villarino, M., Spinola-Amilibia, M., Ruiz-Lopez, E., Illanes Vicioso, R., Castroviejo, P., Aiese Cigliano, R., Montoya, M., Falabella, P., Pesquera, C., Gonzalez-Legarreta, L., Arias-Palomino, E., Sola, M., Torroba, T., Arias, C.F., Bertocchini, F., 2022. Wax worm saliva and the enzymes therein are the key to polyethylene degradation by *Galleria mellonella*. Nat Commun 13, 5568. <https://doi.org/10.1038/s41467-022-33127-w>.
- [23] Bulak, P., Proc, K., Pytlak, A., Puszka, A., Gawdzik, B., Bieganski, A., 2021. Biodegradation of different types of plastics by *Tenebrio molitor* insect. Polymers 13, 3508. <https://doi.org/10.3390/polym13203508>.
- [24] Luo, L., Wang, Y., Guo, H., Yang, Y., Qi, N., Zhao, X., Gao, S., Zhou, A., 2021. Biodegradation of foam plastics by *Zophobas atratus* larvae (Coleoptera: Tenebrionidae) associated with changes of gut digestive enzymes activities and microbiome. Chemosphere 282, 131006. <https://doi.org/10.1016/j.chemosphere.2021.131006>.
- [25] Tsochatzis, E., Alberto Lopes, J., Gika, H., Theodoridis, G., 2020. Polystyrene biodegradation by *Tenebrio molitor* larvae: identification of generated substances using a GC-MS untargeted screening method. Polymers 13, 17. <https://doi.org/10.3390/polym13010017>.
- [26] He, L., Zhang, Y., Ding, M.-Q., Li, M.-X., Ding, J., Bai, S.-W., Wu, Q.-L., Zhao, L., Cao, G.-L., Ren, N.-Q., Yang, S.-S., 2021. Sustainable strategy for lignocellulosic crop wastes reduction by *Tenebrio molitor* linnaeus (mealworm) and potential use of mealworm frass as a fertilizer. J Clean Prod 325, 129301. <https://doi.org/10.1016/j.jclepro.2021.129301>.
- [27] Bovera, F., Piccolo, G., Gasco, L., Marono, S., Loponte, R., Vassalotti, G., Mastellone, V., Lombardi, P., Attia, Y.A., Nizza, A., 2015. Yellow mealworm larvae (*Tenebrio molitor*, L.) as a possible alternative to soybean meal in broiler diets. Br Poult Sci 569–575. <https://doi.org/10.1080/00071668.2015.1080815>.
- [28] Yang, Y., Yang, J., Wu, W.-M., Zhao, J., Song, Y., Gao, L., Yang, R., Jiang, L., 2015. Biodegradation and mineralization of polystyrene by plastic-eating mealworms: Part 2. Role of gut microorganisms. Environ Sci Technol 49, 12087–12093. <https://doi.org/10.1021/acs.est.5b02663>.
- [29] Peng, B.-Y., Sun, Y., Xiao, S., Chen, J., Zhou, X., Wu, W.-M., Zhang, Y., 2022. Influence of polymer size on polystyrene biodegradation in mealworms (*Tenebrio molitor*): Responses of depolymerization pattern, gut microbiome, and metabolome to polymers with low to ultrahigh molecular weight. Environ Sci Technol 23, 17310–17320. <https://doi.org/10.1021/acs.est.2c06260>.
- [30] Tsochatzis, E.D., Berggreen, I.E., Vidal, N.P., Roman, L., Gika, H., Corredig, M., 2022. Cellular lipids and protein alteration during biodegradation of expanded polystyrene by mealworm larvae under different feeding conditions. Chemosphere 300, 134420. <https://doi.org/10.1016/j.chemosphere.2022.134420>.
- [31] Brandon, A., Gao, S., Tian, R., Ning, D., Yang, S., Zhou, J., Wu, W., Criddle, C., 2018. Biodegradation of polyethylene and plastic mixtures in mealworms (larvae of *Tenebrio molitor*) and effects on the gut microbiome. Environ Sci Technol 52, 6526–6533. <https://doi.org/10.1021/acs.est.8b02301>.
- [32] Yang, L., Gao, J., Liu, Y., Zhuang, G., Peng, X., Wu, W.-M., Zhuang, X., 2021. Biodegradation of expanded polystyrene and low-density polyethylene foams in larvae of *Tenebrio molitor* linnaeus (Coleoptera: Tenebrionidae): broad versus limited extent depolymerization and microbe-dependence versus independence. Chemosphere 262, 127818. <https://doi.org/10.1016/j.chemosphere.2020.127818>.
- [33] Yang, S., Ding, M.-Q., Ren, X.-R., Zhang, Z.-R., Li, M.-X., Zhang, L.-L., Pang, J.-W., Chen, C.-X., Zhao, L., Xing, D.-F., Ren, N.-Q., Ding, J., Wu, W.-M., 2022. Impacts of physical-chemical property of polyethylene on depolymerization and biodegradation in yellow and dark mealworms with high purity microplastics. Sci Total Environ 828, 154458. <https://doi.org/10.1016/j.scitotenv.2022.154458>.
- [34] Pham, T.Q., Longin, S., Siebecker, M.G., 2023. Consumption and degradation of different consumer plastics by mealworms (*Tenebrio molitor*): effects of plastic type, time, and mealworm origin. J Clean Prod 403, 136842. <https://doi.org/10.1016/j.jclepro.2023.136842>.
- [35] Yang, S.-S., Ding, M.-Q., He, L., Zhang, C.-H., Li, Q.-X., Xing, D.-F., Cao, G.-L., Zhao, L., Ding, J., Ren, N.-Q., Wu, W.-M., 2021. Biodegradation of polypropylene by yellow mealworms (*Tenebrio molitor*) and superworms (*Zophobas atratus*) via gut-microbe-dependent depolymerization. Sci Total Environ 756, 144087. <https://doi.org/10.1016/j.scitotenv.2020.144087>.
- [36] Liu, J., Liu, J., Xu, B., Xu, A., Cao, S., Wei, R., Zhou, J., Jiang, M., Dong, W., 2022. Biodegradation of polyether-polyurethane foam in yellow mealworms (*Tenebrio molitor*) and effects on the gut microbiome. Chemosphere 304, 135263. <https://doi.org/10.1016/j.chemosphere.2022.135263>.
- [37] Peng, B.-Y., Chen, Z., Chen, J., Zhou, X., Wu, W.-M., Zhang, Y., 2021. Biodegradation of polylactic acid by yellow mealworms (larvae of *Tenebrio molitor*) via resource recovery: a sustainable approach for waste management. J Hazard Mater 416, 125803. <https://doi.org/10.1016/j.jhazmat.2021.125803>.
- [38] He, L., Yang, S.-S., Ding, J., He, Z.-L., Pang, J.-W., Xing, D.-F., Zhao, L., Zheng, H.-S., Ren, N.-Q., Wu, W.-M., 2023. Responses of gut microbiomes to commercial polyester polymer biodegradation in *Tenebrio molitor* larvae. J Hazard Mater 457, 131759. <https://doi.org/10.1016/j.jhazmat.2023.131759>.
- [39] Min, K., Cuiffi, J.D., Mathers, R.T., 2020. Ranking environmental degradation trends of plastic marine debris based on physical properties and molecular structure. Nat Commun 11, 727. <https://doi.org/10.1038/s41467-020-14538-z>.
- [40] Wu, W.-M., Criddle, C.S., 2021. Characterization of biodegradation of plastics in insect larvae. In: Weber, G., Bornscheuer, U.T., Wei, R. (Eds.), Enzym. Plast. Degrad. Elsevier Academic Press Inc, San Diego, pp. 95–120. <https://doi.org/10.1016/bs.mie.2020.12.029>.
- [41] Stehmeier, L.G., Francis, M.M., Jack, T.R., Diegor, E., Winsor, L., Abrajano, T.A., 1999. Field and in vitro evidence for in-situ bioremediation using compound-specific <sup>13</sup>C/<sup>12</sup>C ratio monitoring. Org Geochem 30, 821–833. [https://doi.org/10.1016/S0146-6380\(99\)00065-0](https://doi.org/10.1016/S0146-6380(99)00065-0).
- [42] Cretnik, S., Thoreson, K.A., Bernstein, A., Ebert, K., Buchner, D., Laskov, C., Haderlein, S., Shoukar-Stash, O., Kliegman, S., McNeill, K., Elsner, M., 2013. Reductive dechlorination of TCE by chemical model systems in comparison to dehalogenating bacteria: Insights from dual element isotope analysis (<sup>13</sup>C/<sup>12</sup>C, <sup>37</sup>Cl/<sup>35</sup>Cl). Environ Sci Technol 47, 6855–6863. <https://doi.org/10.1021/es400107n>.
- [43] Liu, Z., Zhao, J., Lu, K., Wang, Z., Yin, L., Zheng, H., Wang, X., Mao, L., Xing, B., 2022. Biodegradation of graphene oxide by insects (*Tenebrio molitor* larvae): Role of the gut microbiome and enzymes. Environ Sci Technol, acs.est.2c03342. <https://doi.org/10.1021/acs.est.2c03342>.
- [44] Suresh Kesti, S., Chandrabanda Thimmappa, S., 2019. First report on biodegradation of low density polyethylene by rice moth larvae, *Coryra cephalonica* (stainton). Holist Approach Environ 9, 79–83. <https://doi.org/10.33765/thate.9.4.2>.
- [45] LeMoine, C.M.R., Grove, H.C., Smith, C.M., Cassone, B.J., 2020. A very hungry caterpillar: polyethylene metabolism and lipid homeostasis in larvae of the greater wax moth (*Galleria mellonella*). Environ Sci Technol 54, 14706–14715. <https://doi.org/10.1021/acs.est.0c04386>.
- [46] Przemienicki, S.W., Kosewska, A., Ciesielski, S., Kosewska, O., 2020. Changes in the gut microbiome and enzymatic profile of *Tenebrio molitor* larvae biodegrading cellulose, polyethylene and polystyrene waste. Environ Pollut 256, 113265. <https://doi.org/10.1016/j.envpol.2019.113265>.
- [47] Brown, J.B., Langley, S.A., Snijders, A.M., Wan, K.H., Morris, S.N.S., Booth, B.W., Fisher, W.W., Hammonds, A.S., Park, S., Weiszmann, R., Yu, C., Kirwan, J.A., Weber, R.J.M., Viant, M.R., Mao, J.-H., Celniker, S.E., 2021. An integrated host-microbiome response to atrazine exposure mediates toxicity in *Drosophila*. Commun Biol 4, 1324. <https://doi.org/10.1038/s42003-021-02847-y>.
- [48] Mamtimin, T., Han, H., Khan, A., Feng, P., Zhang, Q., Ma, X., Fang, Y., Liu, P., Kulshrestha, S., Shigaki, T., Li, X., 2023. Gut microbiome of mealworms (*Tenebrio molitor* larvae) show similar responses to polystyrene and corn straw diets. Microbiome 11, 98. <https://doi.org/10.1186/s40168-023-01550-w>.
- [49] Giebel, B.M., Cime, S., Rodgers, L., Li, T.-D., Zhang, S., Wang, T., 2022. Short-term exposure to soils and sludge induce changes to plastic morphology and <sup>13</sup>C stable isotopic composition. Sci Total Environ 821, 153375. <https://doi.org/10.1016/j.scitotenv.2022.153375>.
- [50] Zhang, G., Liu, D., Lin, J., Kumar, A., Jia, K., Tian, X., Yu, Z., Zhu, B., 2023. Priming effects induced by degradable microplastics in agricultural soils. Soil Biol Biochem 180, 109006. <https://doi.org/10.1016/j.soilbio.2023.109006>.
- [51] Yoshida, S., Hiraga, K., Takehana, T., Taniguchi, I., Yamaji, H., Maeda, Y., Toyohara, K., Miyamoto, K., Kimura, Y., Oda, K., 2016. A bacterium that degrades and assimilates poly(ethylene terephthalate). Science 351, 1196–1199. <https://doi.org/10.1126/science.aad6359>.
- [52] Lou, Y., Li, Y., Lu, B., Liu, Q., Yang, S.-S., Liu, B., Ren, N., Wu, W.-M., Xing, D., 2021. Response of the yellow mealworm (*Tenebrio molitor*) gut microbiome to diet shifts during polystyrene and polyethylene biodegradation. J Hazard Mater 416, 126222. <https://doi.org/10.1016/j.jhazmat.2021.126222>.
- [53] Brandon, A.M., Garcia, A.M., Khlystov, N.A., Wu, W.-M., Criddle, C.S., 2021. Enhanced bioavailability and microbial biodegradation of polystyrene in an enrichment derived from the gut microbiome of *Tenebrio molitor* (mealworm larvae). Environ Sci Technol 55, 2027–2036. <https://doi.org/10.1021/acs.est.0c04952>.

- [54] Genta, F.A., Dillon, R.J., Terra, W.R., Ferreira, C., 2006. Potential role for gut microbiota in cell wall digestion and glucoside detoxification in *Tenebrio molitor* larvae. *J Insect Physiol* 52, 593–601. <https://doi.org/10.1016/j.jinsphys.2006.02.007>.
- [55] Wright, R.J., Bosch, R., Langille, M.G.I., Gibson, M.I., Christie-Oleza, J.A., 2021. A multi-OMIC characterisation of biodegradation and microbial community succession within the PET plastiisphere. *Microbiome* 9, 141. <https://doi.org/10.1186/s40168-021-01054-5>.
- [56] Wei, R., Breite, D., Song, C., Gräsing, D., Ploss, T., Hille, P., Schwerdtfeger, R., Matysik, J., Schulze, A., Zimmermann, W., 2019. Biocatalytic degradation efficiency of postconsumer polyethylene terephthalate packaging determined by their polymer microstructures. *Adv Sci* 6, 1900491. <https://doi.org/10.1002/advs.201900491>.
- [57] Zampolini, J., Orro, A., Manconi, A., Ami, D., Natalello, A., Di Gennaro, P., 2021. Transcriptomic analysis of *Rhodococcus opacus* R7 grown on polyethylene by RNA-seq. *Sci Rep* 11. <https://doi.org/10.1038/s41598-021-00525-x>.
- [58] Gambarini, V., Pantos, O., Kingsbury, J.M., Weaver, L., Handley, K.M., Lear, G., 2021. Phylogenetic distribution of plastic-degrading microorganisms. *mSystems* 6, e0112-20. <https://doi.org/10.1128/mSystems.0112-20>.
- [59] Narciso-Ortiz, L., Coreño-Alonso, A., Mendoza-Olivares, D., Luchó-Constantino, C. A., Lizardi-Jiménez, M.A., 2020. Baseline for plastic and hydrocarbon pollution of rivers, reefs, and sediment on beaches in Veracruz state, México, and a proposal for bioremediation. *Environ Sci Pollut Res* 27, 23035–23047. <https://doi.org/10.1007/s11356-020-08831-z>.
- [60] Sun, C., Zeng, X., Li, G., Du, Y., Wang, Z., Shao, Z., 2021. Diversity of anaerobic degrading bacteria for natural organic polymers in mangrove sediments and isolation of novel groups of bacteria. *Acta Microbiol Sin* 61, 987–1001. <https://doi.org/10.13343/j.cnki.wsxb.20200715>.
- [61] Eisenberg, T., Glaeser, S.P., Kämpfer, P., Schauerte, N., Geiger, C., 2015. Root sepsis associated with insect-dwelling *Sebaldella termittidis* in a lesser dwarf lemur (*Cheirogaleus medius*). *Antonie Van Leeuwenhoek* 108, 1373–1382. <https://doi.org/10.1007/s10482-015-0590-4>.
- [62] Peydai, A., Bagheri, H., Gurevich, L., de Jonge, N., Nielsen, J.L., 2021. Mastication of polyolefin alters the microbial composition in *Galleria mellonella*. *Environ Pollut* 280, 116877. <https://doi.org/10.1016/j.envpol.2021.116877>.
- [63] Pivato, A.F., Miranda, G.M., Prichula, J., Lima, J.E.A., Ligabue, R.A., Seixas, A., Trentin, D.S., 2022. Hydrocarbon-based plastics: progress and perspectives on consumption and biodegradation by insect larvae. *Chemosphere* 293, 133600. <https://doi.org/10.1016/j.chemosphere.2022.133600>.
- [64] Loiret, F.G., Grimm, B., Hajirezaei, M.R., Kleiner, D., Ortega, E., 2009. Inoculation of sugarcane with *Pantoea* sp. increases amino acid contents in shoot tissues; serine, alanine, glutamine and asparagine permit concomitantly ammonium excretion and nitrogenase activity of the bacterium. *J Plant Physiol* 166, 1152–1161. <https://doi.org/10.1016/j.jplph.2009.01.002>.
- [65] Yang, Y., Hu, L., Li, X., Wang, J., Jin, G., 2022. Nitrogen fixation and diazotrophic community in plastic-eating mealworms *Tenebrio molitor* L. *Microb Ecol* 13 (1). <https://doi.org/10.1007/s00248-021-01930-5>.
- [66] Nayakar, A.S., Osuji, E., Carr, D.L., 2023. Gut microbial communities in mealworms and Indianmeal moth larvae respond differently to plastic degradation. *J Polym Environ* 31, 2434–2447. <https://doi.org/10.1007/s10924-023-02773-6>.
- [67] Temporiti, M.E.E., Nicola, L., Nielsen, E., Tosi, S., 2022. Fungal enzymes involved in plastics biodegradation. *Microorganisms* 10, 1180. <https://doi.org/10.3390/microorganisms10061180>.
- [68] Carniel, A., Valoni, É., Nicomedes, J., Gomes, A. da C., Castro, A.M. de, 2017. Lipase from *Candida antarctica* (CALB) and cutinase from *Humicola insolens* act synergistically for PET hydrolysis to terephthalic acid. *Process Biochem* 59, 84–90. <https://doi.org/10.1016/j.procbio.2016.07.023>.
- [69] Billig, S., Oeser, T., Birkemeyer, C., Zimmermann, W., 2010. Hydrolysis of cyclic poly(ethylene terephthalate) trimers by a carboxylesterase from *Thermobifida fusca* KW3. *Appl Microbiol Biotechnol* 87, 1753–1764. <https://doi.org/10.1007/s00253-010-2635-y>.
- [70] Wei, R., Zimmermann, W., 2017. Microbial enzymes for the recycling of recalcitrant petroleum-based plastics: How far are we? *Microb Biotechnol* 10, 1308–1322. <https://doi.org/10.1111/1751-7915.12710>.
- [71] Giangeri, G., Morlino, M.S., De Bernardini, N., Ji, M., Bosaro, M., Pirillo, V., Antoniali, P., Molla, G., Raga, R., Treu, L., Campanaro, S., 2022. Preliminary investigation of microorganisms potentially involved in microplastics degradation using an integrated metagenomic and biochemical approach. *Sci Total Environ* 843, 157017. <https://doi.org/10.1016/j.scitotenv.2022.157017>.
- [72] Jahanshahi, D.A., Ariaeenejad, S., Kavousi, K., 2023. A metagenomic catalog for exploring the plastizymes landscape covering taxa, genes, and proteins. *Sci Rep* 13 (1), 14. <https://doi.org/10.1038/s41598-023-43042-9>.
- [73] Luo, C., Li, Y., Chen, Y., Fu, C., Long, W., Xiao, X., Liao, H., Yang, Y., 2019. Bamboo lignocellulose degradation by gut symbiotic microbiota of the bamboo snout beetle *Cyrtotrachelus buqueti*. *Biotechnol Biofuels* 12, 70. <https://doi.org/10.1186/s13068-019-1411-1>.
- [74] Gyung Yoon, M., Jeong Jeon, H., Nam Kim, M., 2012. Biodegradation of polyethylene by a soil bacterium and AlkB cloned recombinant cell. *J Bioremediation Biodegrad* 03. <https://doi.org/10.4172/2155-6199.1000145>.
- [75] Lacal, J., Muñoz-Martínez, F., Reyes-Darfás, J.-A., Duque, E., Matilla, M., Segura, A., Calvo, J.-J.O., Jiménez-Sánchez, C., Krell, T., Ramos, J.L., 2011. Bacterial chemotaxis towards aromatic hydrocarbons in *Pseudomonas*. *Environ Microbiol* 13, 1733–1744. <https://doi.org/10.1111/j.1462-2920.2011.02493.x>.
- [76] Gravouil, K., Ferru-Clement, R., Colas, S., Helye, R., Kadri, L., Bourdeau, L., Moumen, B., Mercier, A., Ferreira, T., 2017. Transcriptomics and lipidomics of the environmental strain *Rhodococcus ruber* point out consumption pathways and potential metabolic bottlenecks for polyethylene degradation. *Environ Sci Technol* 51, 5172–5181. <https://doi.org/10.1021/acs.est.7b00846>.
- [77] Vera-Ponce de León, A., Ormeño-Orrillo, E., Ramírez-Puebla, S.T., Rosenblueth, M., Degli Esposti, M., Martínez-Romero, J., Martínez-Romero, E., 2017. *Candidatus Dactylopiibacterium carminicum*, a nitrogen-fixing symbiont of *Dactylopius* cochineal insects (Hemiptera: Coccoidea: Dactylopiidae). *Genome Biol Evol* 9, 2237–2250. <https://doi.org/10.1093/gbe/exv156>.
- [78] Terra, W.R., Barroso, I.G., Dias, R.O., Ferreira, C., 2019. Molecular physiology of insect midgut. *Advances in Insect Physiology*. Elsevier, pp. 117–163. <https://doi.org/10.1016/bs.aiip.2019.01.004>.
- [79] Ahmaditabatabaei, S., Kyazze, G., Iqbal, H.M.N., Keshavarz, T., 2021. Fungal enzymes as catalytic tools for polyethylene terephthalate (PET) degradation. *J Fungi* 7, 931. <https://doi.org/10.3390/jof7110931>.
- [80] Liu, S., Shi, X.-X., Jiang, Y.-D., Zhu, Z.-J., Qian, P., Zhang, M.-J., Yu, H., Zhu, Q.-Z., Gong, Z.-J., Zhu, Z.-R., 2015. De novo analysis of the *Tenebrio molitor* (Coleoptera: Tenebrionidae) transcriptome and identification of putative glutathione S-transferase genes. *Appl Entomol Zool* 50, 63–71. <https://doi.org/10.1007/s13355-014-0305-8>.
- [81] Katewa, S.D., Demontis, F., Kolipinski, M., Hubbard, A., Gill, M.S., Perrimon, N., Melov, S., Kapahi, P., 2012. Intramycellular fatty-acid metabolism plays a critical role in mediating responses to dietary restriction in *Drosophila melanogaster*. *Cell Metab* 16, 97–103. <https://doi.org/10.1016/j.cmet.2012.06.005>.
- [82] Xu, G., Yu, Y., 2021. Polystyrene microplastics impact the occurrence of antibiotic resistance genes in earthworms by size-dependent toxic effects. *J Hazard Mater* 416, 125847. <https://doi.org/10.1016/j.jhazmat.2021.125847>.
- [83] Moreira, N.R., Cardoso, C., Dias, R.O., Ferreira, C., Terra, W.R., 2017. A physiologically-oriented transcriptomic analysis of the midgut of *Tenebrio molitor*. *J Insect Physiol* 99, 58–66. <https://doi.org/10.1016/j.jinsphys.2017.03.009>.
- [84] Gewert, B., Plassmann, M.M., MacLeod, M., 2015. Pathways for degradation of plastic polymers floating in the marine environment. *Environ Sci Process Impacts* 17, 1513–1521. <https://doi.org/10.1039/C5EM00207A>.
- [85] Kawai, F., Kawabata, T., Oda, M., 2019. Current knowledge on enzymatic PET degradation and its possible application to waste stream management and other fields. *Appl Microbiol Biotechnol* 103, 4253–4268. <https://doi.org/10.1007/s00253-019-09717-y>.